Synthesis and Structure of Arene Ru(II) N^O-Chelating Complexes: *In Vitro* Cytotoxicity and Cancer Cell Death Mechanism

Sundarraman Balaji[a], Mohamed Kasim Mohamed Subarkhan[b], Rengan Ramesh[a*], Hangxiang Wang[b], David Semeril[c]

[a]Centre for Organometallic Chemistry, School of Chemistry, Bharathidasan University, Tiruchirappalli – 620 024, India.

[E-mail: ramesh_bdu@yahoo.com and phone No. 0431- 2407053; Fax: 0091-431-2407045]

[b]The First Affiliated Hospital, Key Laboratory of Combined Multi-Organ Transplantation, Ministry of Public Health, School of Medicine, Zhejiang University, Hangzhou, 310003, PR China.

[c]Laboratoire de Chimie Inorganique et Catalyse, Institut de Chimie, Universite de Strasbourg, UMR 7177, CNRS, France.

*To whom correspondence should be made: Tel: +91-431-2407053, Fax: +91-431-2407045, E-mail: ramesh_bdu@yahoo.com

CONTENTS

Materials, Methodsand Crystal data collection

The starting materials $[(\eta^6\text{-}p\text{-cymene})RuCl_2]_2$ and $[(\eta^6\text{-benzene})RuCl_2]_2$ were prepared by literature methods.[1,2] Chemically pure and analar gradereagents were used for all the reactions. Commercially available $RuCl_3.3H_2O$ was used as received from Loba Chemie. 4-chloro, 4-methoxy, unsubstituted benzhydrazides and 4-(dimethylamino)benzaldehyde were purchased from Sigma Aldrich. The solvents were freshly distilled before use by following standard procedures.[3] Boeties micro heating table was used to record the melting points and are uncorrected. The analysis of carbon, hydrogen, nitrogen and sulphur were performed at Sophisticated Test and Instrumentation Centre (STIC), Cochin University of Science and Technology, Kochi. Perkin-Elmer 597 spectrophotometer was utilized to record the IR spectra of ligands and complexes were with KBr pellets with a in the range of 4000-400 cm^{-1}. A Cary 300 Bio UV–vis Varian spectrophotometer was used to record the electronic spectra of complexes in the range 800-200 nm. The ^{1}H-NMR spectra were recorded with Bruker 400 MHz instrument using TMS as internal referencein $CDCl_3$. A Micro mass thermoscientific LTQ XL mass spectrometer was utilized for High Resolution Mass Spectrometry of the complexes.

Single crystals of complexes **1** and **4** were grown by slow evaporation of a dichloromethane in petroleum ether solution at room temperature. A single crystal of suitable size was covered with Paratone oil, mounted on the top of a glass fiber, and transferred to a Bruker AXS Kappa APEX II single crystal X-ray diffractometer using monochromated MoKα radiation (λ = 0.71073). Data were collected at 293 K. The structure was solved by direct methods using SIR-97 and was refined by the full matrix least-squares method on F^2 with SHELXL-97.[4] Non-hydrogen atoms were refined with anisotropy thermal parameters. All hydrogen atoms were geometrically fixed and collected to refine using a riding model. Frame integration and data reduction were performed using the Bruker SAINT Plus (Version 7.06a) software. The multiscan absorption corrections were applied to the data using SADABS software.[5] Figures 3 and 4 was drawn with ORTEP and the structural data have been deposited at the Cambridge Crystallographic Data Centre: CCDC **1833167** and **1565996**.

Stability studies

UV-visible time dependent spectral method has been used to examine the stability of the complexes. Complexes were dissolved in a minimum amount of 1% DMSO and then diluted with PBS buffer to 1×10^{-3} M concentration. The hydrolysis profiles of the complexes were monitored by their electronic spectra over 72 h.

Partition coefficients determination

The lipophilicity of complexes **1−6** was determined by the "shake flask" method between octanol/water phase partitions. Octanol-saturated water (OSW) and water-saturated octanol (WSO) were prepared using analytical grade octanol (Sigma Aldrich) and doubly distilled water. Complexes **1−6** (1 mg/mL; ethanol/water 1/6) were diluted to 2, 4, 6, 8, and 10 μg/mL in water; alternatively these (1 mg/mL) were diluted to 2, 4, 6, 8, and 10 μg/mL in octanol, respectively. Appropriate amounts of the complexes (4 mg/mL) were shaken for 24 h at room temperature in equal volume (50/50). After the attainment of equilibrium, the organic and aqueous phases were separated and centrifuged. Finally, the concentration of the drug in each phase was determined by UV-visible spectroscopy. The sample solution concentration was used to calculate log P. Partition coefficients for complexes **1−6** were calculated using the equation log P = log[(1−6)oct/(1−6)aq].[6]

Cell culture

A549, LoVo, HuH-7 and 16HBE cells were purchased from the cell bank of the Chinese Academy of Sciences (Shanghai, China). A549 and LoVo cells were cultured in RPMI-1640 (Gibco) supplemented with 10% fetal bovine serum (FBS; Gibco). HuH-7 and 16HBE cells were cultured in Dulbecco's modified Eagle's medium (DMEM). All of themedia were supplemented with 10% fetal bovineserum (FBS), penicillin (100 units/mL) andstreptomycin (100 μg/mL), and the cells weremaintained in a humid atmosphere at 37 °C with 5%CO_2.

In vitro cytotoxicity using an MTT assay

The in vitro cytotoxicity of the complexes was measured by an MTT (3-(4,5-dimethylthiazol-2-yl)-2,5-diphenyltetrazolium bromide) assay. The cellswere plated in flat-bottomed 96-well plates (4×10^3 cells per well) and incubated at 37 °C for 24 h. Thecells were added via serial dilution of Complexes **1-6** and cisplatin and then incubated at 37 °C for 72 h. At the end of the exposure, 30 μLMTT solution (5 mg/mL in PBS) was added to eachwell. The MTT solution was removed from the wellsafter 4 h, and the purple MTT-formazan crystals werethen dissolved by the addition of DMSO (100 μL). Theabsorbance in each well was measured at 490 nmusing a microplate reader (Multiskan FC, ThermoScientific). DMSO blank assay has been performed before all cell assays.

EdU assay

2×10^4 of A549 cells were seeded into 48-well plates with per well and hatched at 37 °C under a 5% CO_2 atmosphere for 24 h. Complexes **4-6** and cisplatin (3.5 μM, equiv concentrations)were then added to the cells and incubated for an additional 24 h at 37 °C. At the end of the drug treatment DNA synthesis were measured using Alexa Fluor 488 Assay Kit (Invitrogen)Click-iT EdU. Click-iT EdU added and incubated 2 h at room temperature. After the A549 cells were fixed with 4% formaldehyde for 15 min, then 0.5% Triton X-100 was added into the A549 cells and incubated with 10 min. Later, azide labeled Alexa Fluor 488 was added into the A549 cells and incubated 30 min at dark condition. After 30 min later, staining the nuclei with Hoechst 33342 (Invitrogen) for 15 min, the cells were imaged using fluorescence microscopy (Olympus, IX71).

Acridine orange-ethidium bromide (AO-EB) staining

4×10^3 of A549 cells were seeded in 24-well plates and incubated at 37 °C for 24 h. Complexes **4-6** and cisplatin (3.5 μM, equiv concentrations) were incubated with A549 cells. After incubation24 h, AO (100 μg/mL) and EB (100 μg/mL) was added to each well (500 μL). After 5 min later, the cells were visualized via a fluorescence microscope (Olympus, BX-60, Japan), and the cell death were measured three random fields of the microscope.

Flow cytometry/Annexin V-PI staining

The flow cytometry analysis with the fluoresceinisothiocyanate (FITC) Annexin V Apoptosis Detection Kit (Multi Sciences, China) used to determine the A549 cells apoptotic ratio. The cells were composed by trypsinization, and washed with twice and resuspended in 500 μL 1 × binding buffer with 5 μL of FITC Annexin V and 10 μL of PI. After 15 min, the samples were subjected to analysis by flow cytometry. The outcomes were analysed with the BD FACS Calibur™ system.

Cell cycle analysis

A549 cells were seeded into 6 well plates incubated, and allowed to attach for 24 h. Then, fresh media containing 3.5 μM complexes **4-6** and cisplatin were added and further incubated for another 24 h. The untreated cells were included as the control. After drug treatment, the cells were centrifuged at 1000 RPM for 5 min and washed with cold PBS. The cells were fixed with 75% ethanol at 4 °C overnight. The cells were then collected and washed twice with PBS. Thereafter, the cells were stained with a solution containing PI (50 μg/mL) and incubated 30 min in the dark condition. Cell cycle distribution was then analysed with a BD FACSCanto™ II flow cytometer.

Western blot analysis

A549 cells were treated with complex **6** (1, 2 and 3 μM concentrations) for 24 h, and appropriate amounts of the cell lysates were resolved over a 10% Tris-glycine polyacrylamide gel, and then transferred onto the PVDF membrane. The blots were blocked using 5% non-fat dry milk and probed using BCL-2 and BAX primary monoclonal antibodies in blocking buffer overnight at 4 ^{o}C. The membrane was then incubated with the appropriate secondary antibody-horseradish peroxidase conjugate (Cell Signaling Technology, China), followed by detection using a chemiluminescence ECL kit (Cell Signaling Technology, China). To ensure equal loading of the protein, the membrane was stripped and reprobed with GAPDH antibody.

Experimental data of benzhydrazone ligands:

HL1 (R = H):Colour: White solid; Yield: 91%, M.p.: 164°C; Anal. Calc. for $C_{16}H_{17}N_3O$ (290.32 g mol^{-1}): C, 71.85; H, 6.44; N, 15.75. Found: C, 71.88; H, 6.40; N, 15.72. IR (KBr, cm^{-1}): 1546 $\nu_{(HC=N)}$, 3427$\nu_{(N-H)}$, 1661 $\nu_{(C=O)}$^{1}H NMR (400 MHz, $CDCl_3$) (ppm): 10.29 (s, 1H, NH), 8.27 (s, 1H, CH=N), 7.89 (d, ^{3}J = 8 Hz, H12, H16), 7.57 (d, ^{3}J = 8 Hz, H3, H5), 7.38 (m, H13, H14, H15), 6.56 (d, ^{3}J = 4 Hz, H2, H6) 2.92 (s, 6H,N$(CH_3)_2$). ^{13}C{1H} NMR (100 MHz, $CDCl_3$) (δ ppm): 164.3 (N–C=O), 151.8 (C-N$(CH_3)_2$), 149.8 (HC=N), 133.6 (Ar^{C11}), 131.6 (Ar^{C14}), 129.4 ($Ar^{C13,C15}$), 128.5 ($Ar^{C3,C5}$), 127.5 ($Ar^{C12,C16}$), 121.4 (Ar^{C4}),111.6 ($Ar^{C2,C6}$), 40.1 (N$(CH_3)_2$).

HL2 (R = Cl): Colour: Pale-Yellow; Yield: 87%; M.p.: 166°C; Anal. Calc. for $C_{16}H_{16}ClN_3O$ (324.76 g mol^{-1}): C, 63.62; H, 5.36; N, 13.96. Found: C, 63.67; H, 5.34; N, 13.92. IR (KBr, cm^{-1}): 1598$\nu_{(HC=N)}$, 3462$\nu_{(N-H)}$, 1653$\nu_{(C=O)}$. ^{1}H NMR (400 MHz, DMSO-d_6) (ppm): 11.55 (s, 1H, NH), 8.21 (s, 1H, CH=N), 7.84 (d, ^{3}J = 8 Hz, H12, H16), 7.49 (dd, ^{3}J = 16, 8 Hz, H3, H5, H13, H15), 6.68 (d, ^{3}J = 8 Hz, H2, H6), 2.89 (s, 6H, N$(CH_3)_2$). ^{13}C{1H} NMR (100 MHz, DMSO-d_6) (δ ppm): 161.6 (N–C=O), 151.5 (C-N$(CH_3)_2$), 148.9 (HC=N), 136.2 (Ar^{C14}), 132.4 (Ar^{C11}), 129.3 ($Ar^{C13,C15}$), 128.5 ($Ar^{C3,C5}$), 121.3 (Ar^{C4}), 111.7 ($Ar^{C2,C6}$), 39.7 (N$(CH_3)_2$).

HL3 (R = OMe): Colour: White solid; Yield: 89%, M.p.: 169°C; Anal. Calc. for $C_{17}H_{19}N_3O_2$ (369.21 g mol^{-1}): C, 58.56; H, 3.55; N, 7.59. Found: C, 58.63; H, 3.59; N, 7.63. IR (KBr, cm^{-1}): 1601 $\nu_{(HC=N),}$ 3242$\nu_{(N-H)}$, 1656 s $\nu_{(C=O)}$^{1}H NMR (400 MHz, DMSO-d_6) (ppm): 11.46 (s, 1H, NH), 8.31 (s, 1H, CH=N), 7.90 (d, ^{3}J = 4 Hz, H12, H16), 7.54 (d, ^{3}J = 8 Hz, H3, H5), 7.05 (d, ^{3}J = 4 Hz, H13, H15), 6.75 (d, ^{3}J = 8 Hz, H2, H6), 3.83(s, 3H, OCH_3), 2.96 (s, 6H, N$(CH_3)_2$). ^{13}C{^{1}H} NMR (100 MHz, DMSO-d_6) (δ ppm): 162.1 (Ar^{C14}), 161.7 (N–C=O), 151.3 (C-N$(CH_3)_2$), 148.0 (HC=N), 129.3 ($Ar^{C12,C16}$), 128.2 ($Ar^{C3,C5}$), 125.8 (Ar^{C11}), 121.7 (Ar^{C4}), 113.6 ($Ar^{C13,C15}$), 111.7 ($Ar^{C2,C6}$), 55.3 (OCH_3), 39.6 (N$(CH_3)_2$).

Table S1. Crystal data and structure refinement for complex **1 and 4.**

Crystal data	**Complex 1**	**Complex 4**
Empirical formula	$C_{22}H_{22}N_3OClRu$	$C_{26}H_{30}N_3OClRu$
Formula weight	480.94	537.11
Colour	Brown	Red-Brown
CCDC number	1833167	1565996
Temperature (K)	173(2)	173(2)
Wavelength (Å)	0.71073	0.71073
Crystal system	orthorhombic	monoclinic
Space group	'Pbca'	'P 2_1/c'
a (Å)	13.6277(2)	15.6788(4)
b (Å)	13.2265(2)	7.5556(2)
c (Å)	23.0153(3)	21.3824(4)
α (°)	90	90
β (°)	90	107.5040(10)
γ (°)	90	90
Volume (Å^3)	4148.43(10)	2415.73(10)
Z	8	4
Crystal_density $\rho_{calcd.}$ (Mg m^{-3})	1.540	1.477
Absorption coefficient(μ) (mm^{-1})	0.902	0.783
F(000)	1952	1104
Crystal size (mm)	0.35×0.28×0.18	0.20 × 0.12× 0.10
Theta range (°)	1.770 to 27.493	1.362 to 27.487
Limiting indices	h = 16< = h < = -17 k = 17 < = k < = -17 l = 27 < = l < = - 29	h = 20< = h < = -20 k = 9 < = k < = -9 l = 27 < = l < = - 27
Reflections collected/unique	43430/4756	38764/5536
Data/restraints/parameters Goodness-of – fit on F^2	4756/0/250 1.131	5536/0/295 1.122
Final *R* indices [I>2σ(I)] *R* indices (all data) Largest diff. Peak and hole(e ^{o}A^{-3})	 0.0550, 0.0414 0.1218, 0.1084	 0.0931, 0.0513 0.1434, 0.1106

Table S2. Selected bond lengths (Å) and angles (°) for the complexes **1** and **4.**

Complex **1**		Complex **4**	
N(2)-Ru(1)	2.112(3)	N(1) Ru(1)	2.096(3)
O(1)-Ru(1)	2.060(2)	O(1)-Ru(1)	2.054(2)
Cl(1)- Ru(1)	2.4116(9)	Cl(1)-Ru(1)	2.4028(11)
N(1)-N(2)	1.405(3)	N(1)-N(2)	1.418(4)
C(7)- N(1)	1.309(4)	C(7)-N(1)	1.295(5)
C(7)-O(1)	1.296(4)	C(10)-N(2)	1.303(5)
C(8)-N(2)	1.286(4)	C(10)-O(1)	1.297(5)
C(22)-Ru(1)	2.194(7)	C(22)-Ru(1)	2.212(4)
*$Centroid_{Ru\text{-}benzene}$	1.656	$Centroid_{Ru\text{-}Cymene}$	1.677
*$Centroid_{metallacycle}$-Ru-$Centroid_{arene(benzene)}$	89.2	$Centroid_{metallacycle}$-Ru-$Centroid_{arene(cymene)}$ =	86.25
*$Centroid_{arene(benzene)}$-Ru-Cl	127.56	$Centroid_{arene(cymene)}$-Ru-Cl	129.82
O(1)-Ru(1)- N(2)	76.74(9)	O(1)-Ru(1)-N(1)	76.73(12)
N(2)-Ru(1)-C(20)	100.7(2)	N(1)-Ru(1)-C(20)	110.68(14)
O(1)-Ru(1)-C(20)	101.6(2)	O(1)-Ru(1)-C(20)	93.03(14)
C(7)-O(1)-Ru(1)	112.06(18)	C(10)-O(1)-Ru(1)	112.4(2)
O(1)-Ru(1)-Cl(1)	85.99(6)	O(1)-Ru(1)-Cl(1)	84.89(8)
N(2)-Ru(1)-Cl(1)	88.79(7)	N(1) Ru(1) Cl(1)	85.88(10)
O(1)-C(7)-N(1)	125.6(3)	O(1)-C(10)-N(2)	125.7(4)
C(7)-N(1)-N(2)	111.4(3)	C(7)-N(1)-N(2)	112.5(3)
C(8)-N(2)-N(1)	114.1(3)	C(10)-N(2)-N(1)	110.7(3)

*In both the complexes, the arene ring and ruthenium ion were seated away from the chloride ion which is evident from the bond angles $Centroid_{metallacycle}$-Ru-$Centroid_{benzene}$ = 89.2°; $Centroid_{benzene}$-Ru-Cl = 127.56°; $Centroid_{metallacycle}$-Ru-$Centroid_{cymene}$ = 86.25°; $Centroid_{cymene}$-Ru-Cl = 129.82°. The Ru(II) ion is sandwiched between the two planes defined by arene ring and the N, O and Cl atoms. The Ru(II) ion is seated away from the plane of the three legs constituted by N, O and Cl atoms by a distance 1.389 Å ($plane_{N,O,Cl}$-$Ru(II)_{arene(benzene)}$) and 1.409 Å ($plane_{N,O,Cl}$-$Ru(II)_{arene(cymene)}$). Since the dihedral angle between the two planes is 6° ($plane_{N,O,Cl}$-$plane_{Ru(II)arene(benzene)}$) and 6.60° ($plane_{N,O,Cl}$-$plane_{Ru(II)arene(cymene)}$), the Ru(II) ion adopted distorted octahedral geometry.

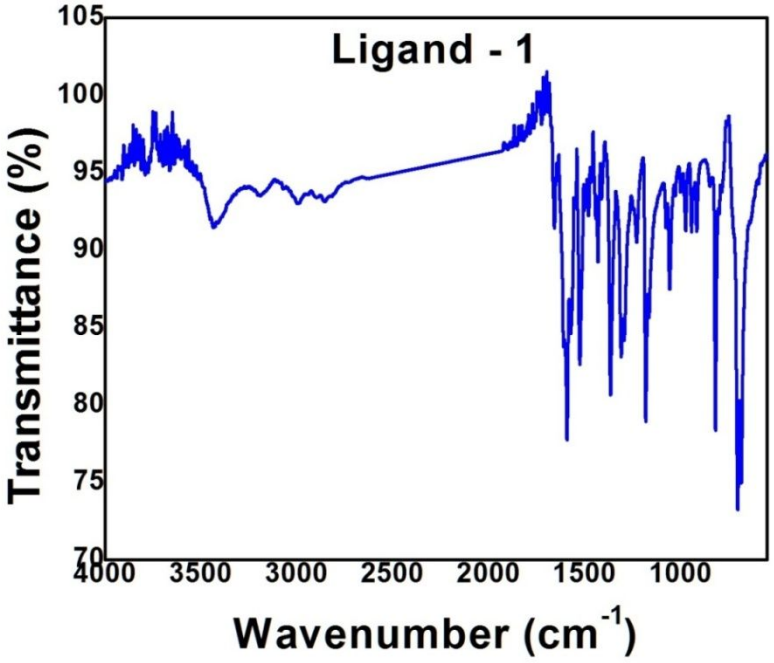

Figure S1. FT-IR spectrum of HL1 [Wavenumber (cm^{-1}): ν_{N-H}(3427), $\nu_{CH=N}$(1546), $\nu_{C=O}$(1661)].

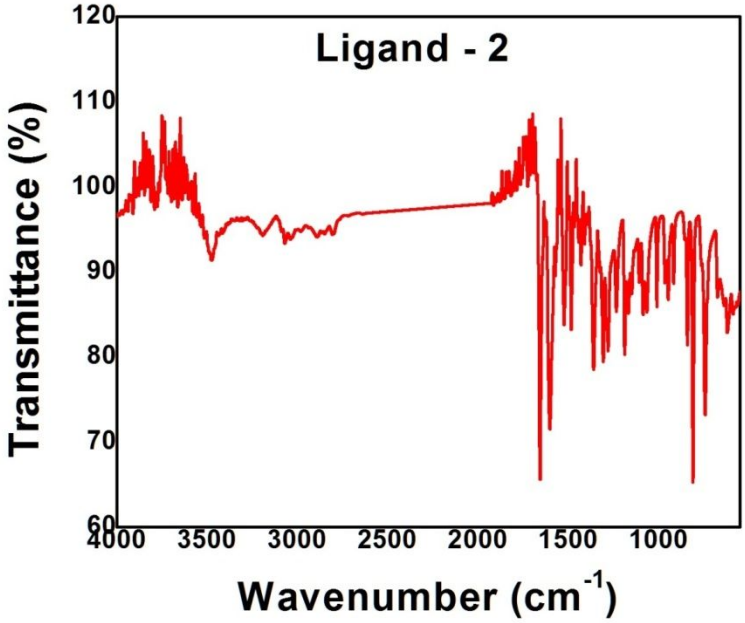

Figure S2. FT-IR spectrum of HL2 [Wavenumber (cm^{-1}): ν_{N-H}(3462), $\nu_{CH=N}$(1598), $\nu_{C=O}$(1653)].

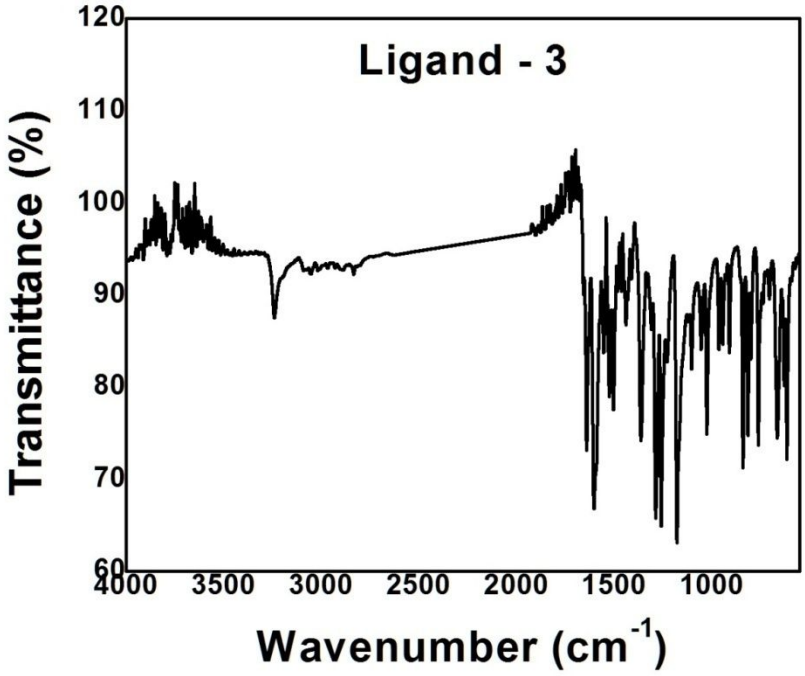

Figure S3. FT-IR spectrum of HL3 [Wavenumber (cm^{-1}): ν_{N-H}(3242), $\nu_{CH=N}$(1601), $\nu_{C=O}$(1656)].

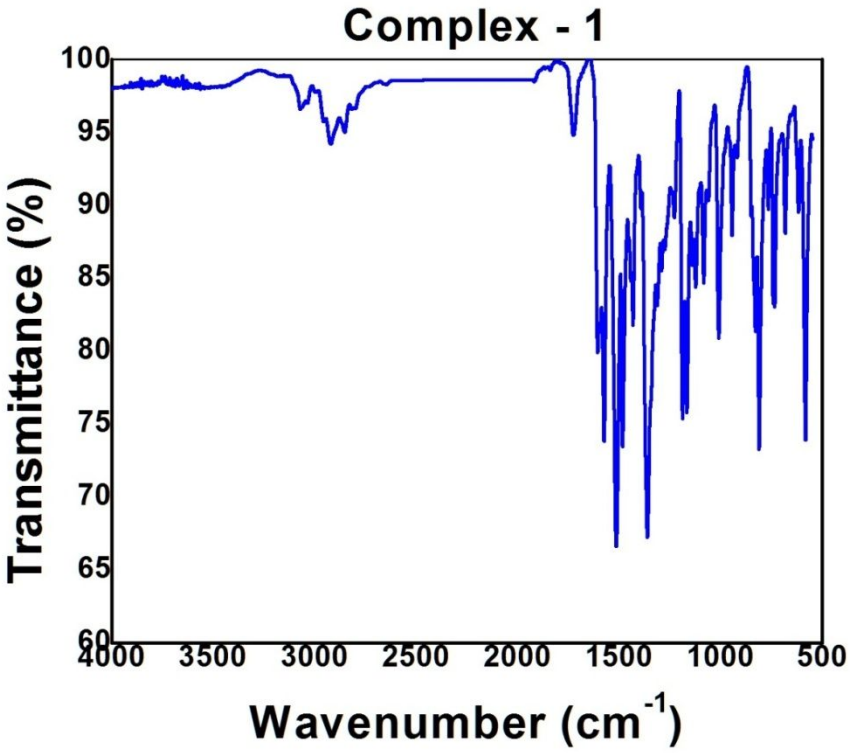

Figure S4. FT-IR spectrum of complex **1**[Wavenumber (cm^{-1}): $\nu_{CH=N}$(1512), ν_{C-O}(1362)].

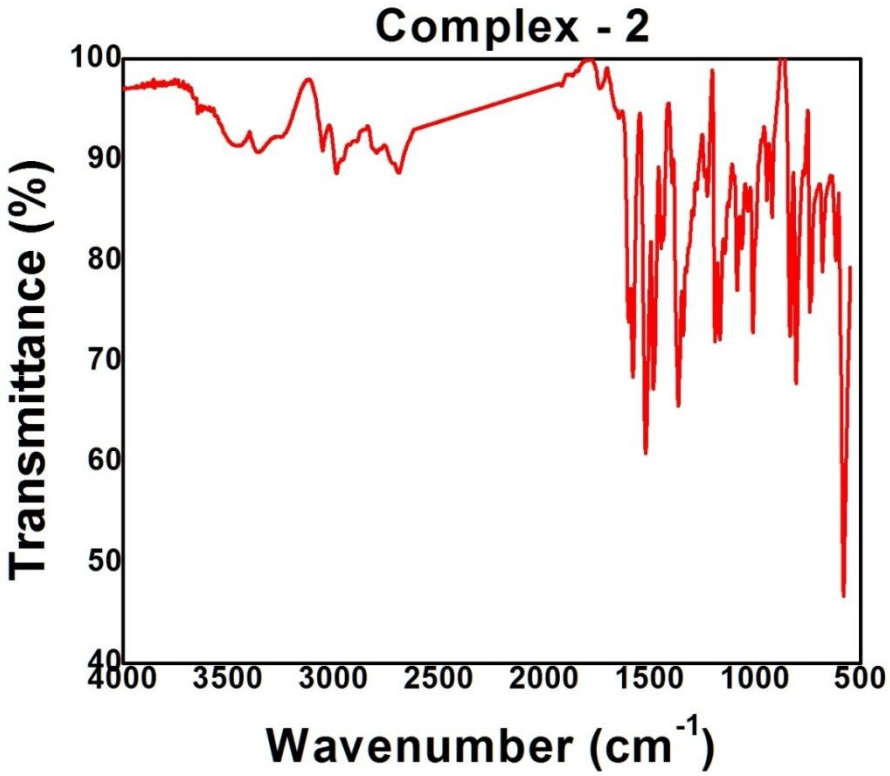

Figure S5. FT-IR spectrum of complex **2** [Wavenumber (cm^{-1}): $\nu_{CH=N}$(1530) ν_{C-O}(1366)].

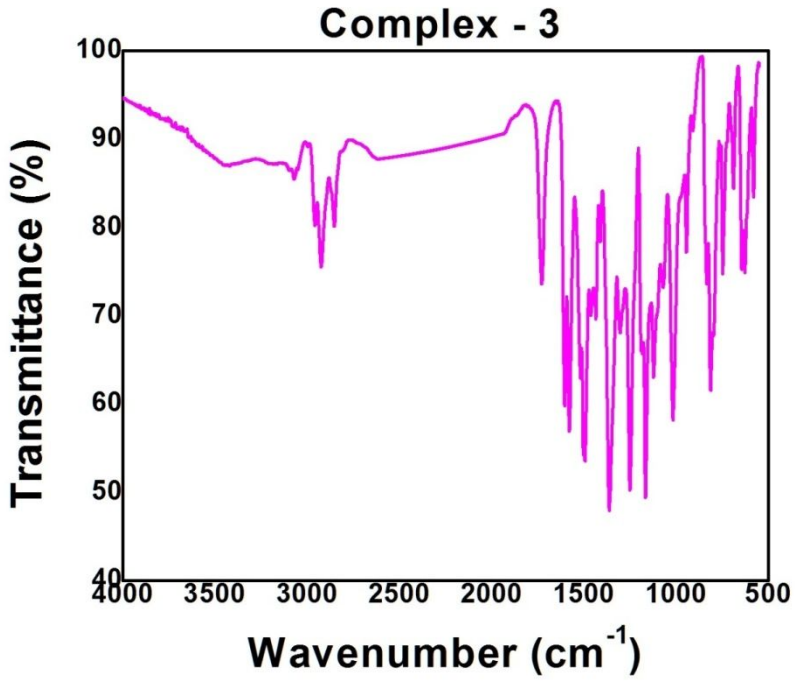

Figure S6. FT-IR spectrum of complex **3** [Wavenumber (cm^{-1}): $\nu_{CH=N}$(1500), ν_{C-O}(1363)].

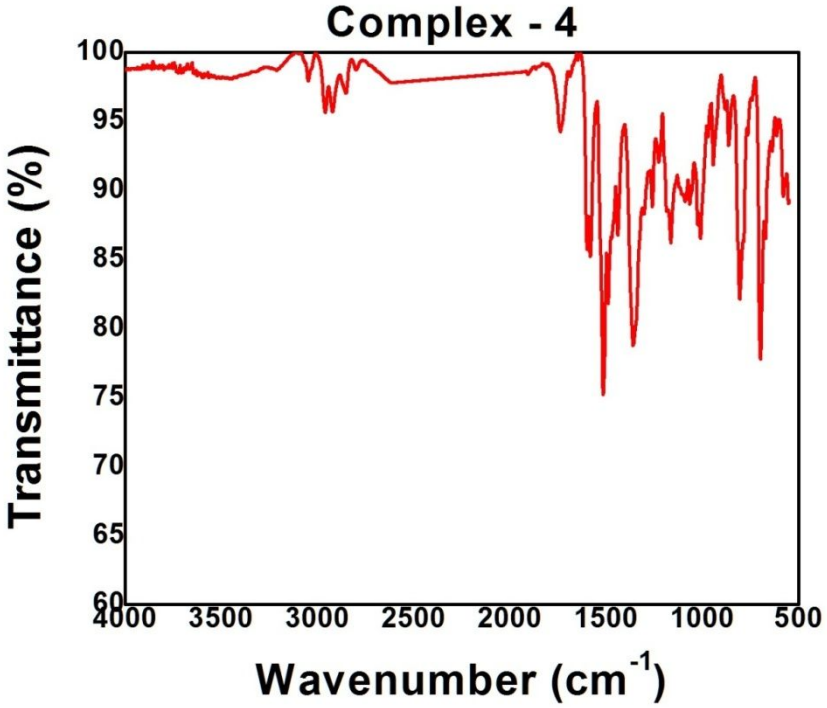

Figure S7. FT-IR spectrum of complex **4** [Wavenumber (cm^{-1}): $\nu_{CH=N}$(1516), ν_{C-O}(1361)].

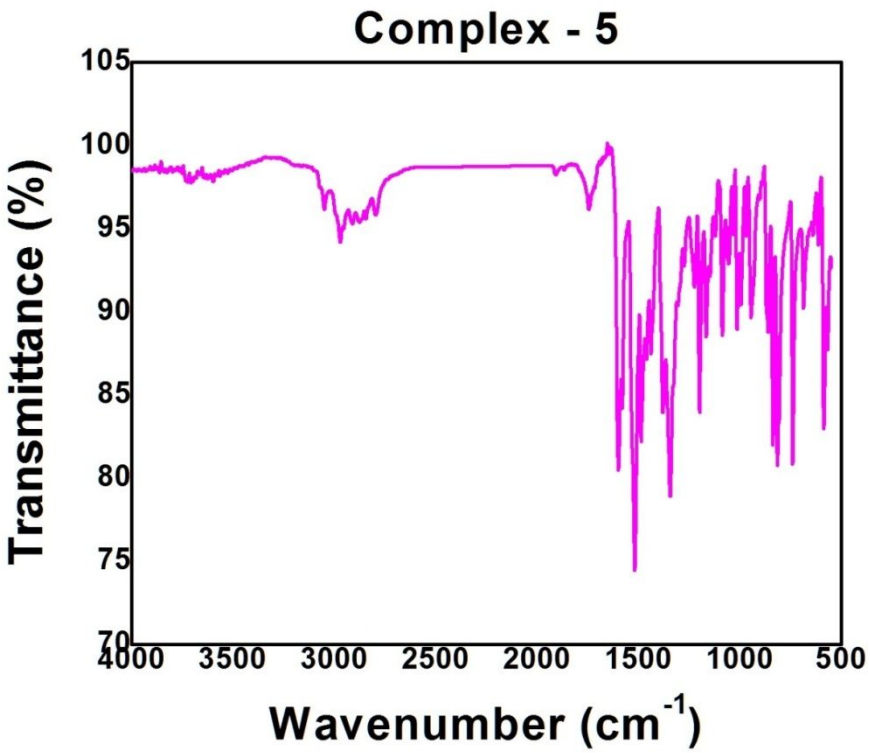

Figure S8. FT-IR spectrum of complex **5** [Wavenumber (cm^{-1}): $\nu_{CH=N}$(1519), ν_{C-O}(1340)].

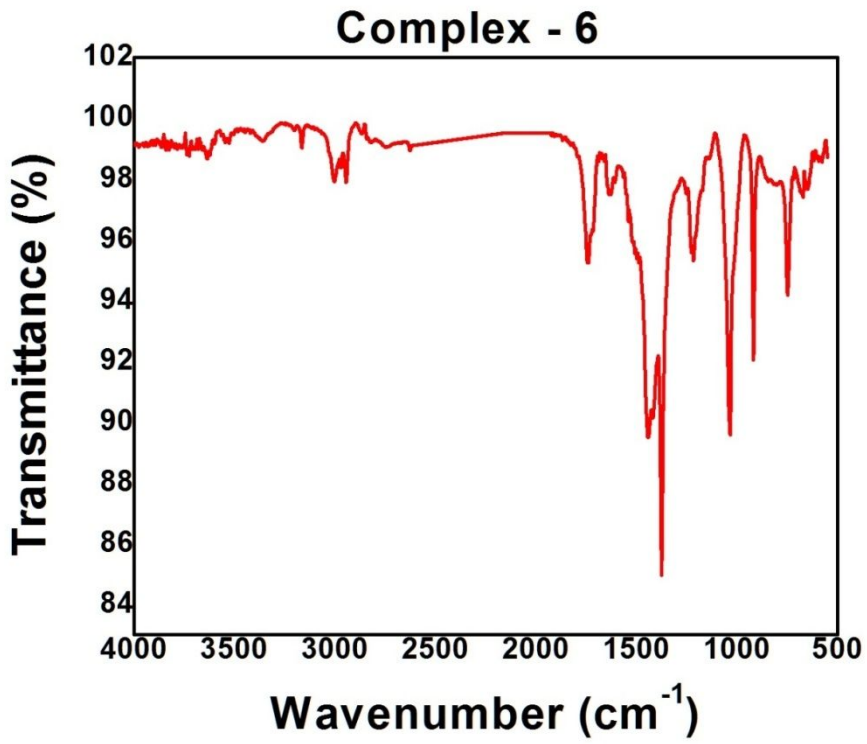

Figure S9. FT-IR spectrum of complex **6** [Wavenumber (cm^{-1}): $\nu_{CH=N}$(1508), ν_{C-O}(1370)].

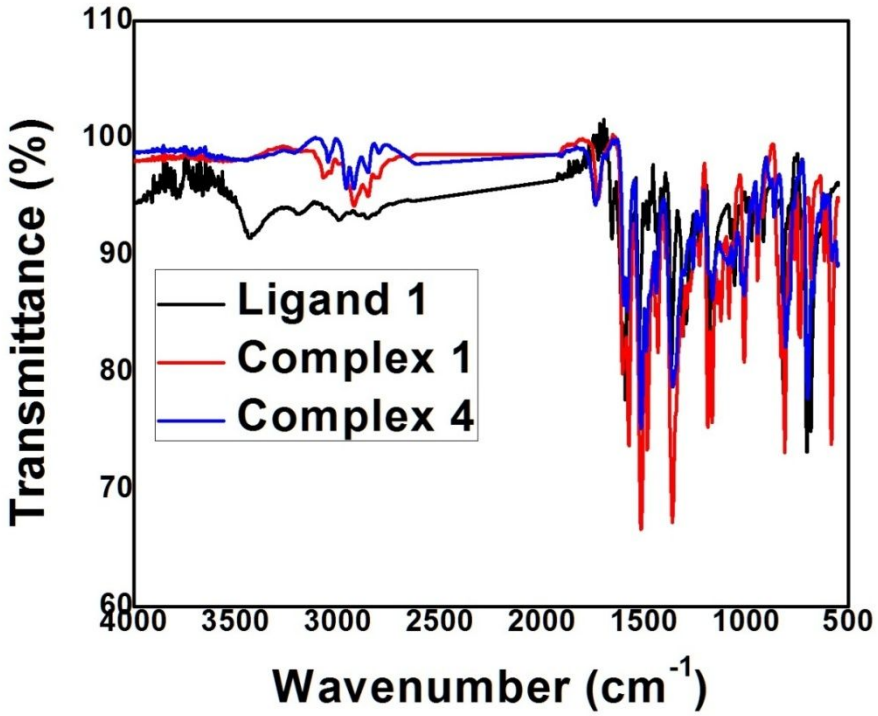

Figure S10. Overlaid FT-IR spectrum of HL1 with complex **1** and **4**.

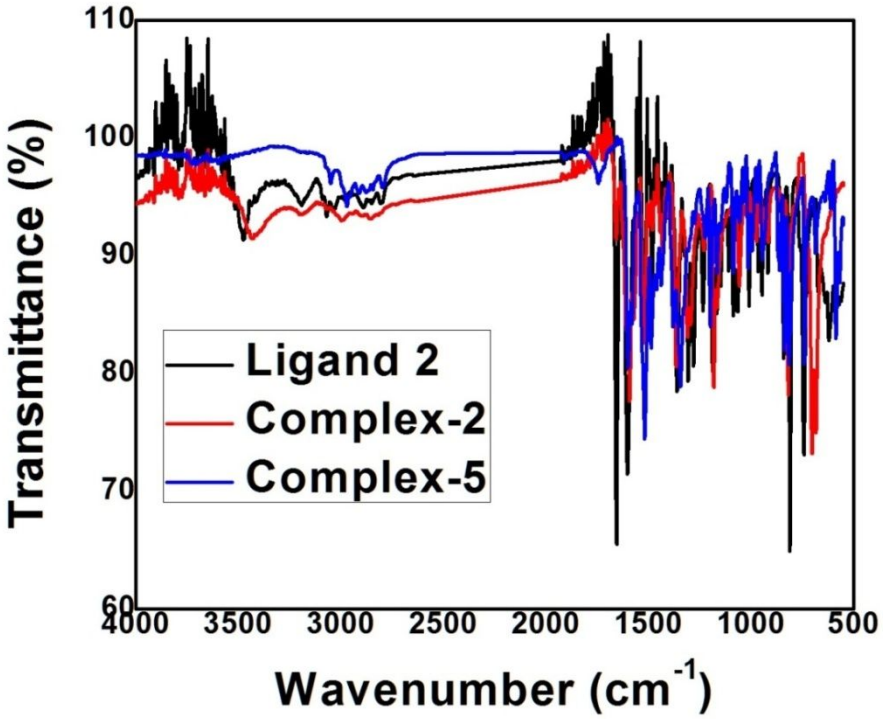

Figure S11. Overlaid FT-IR spectrumof HL2 withcomplex **2** and **5**.

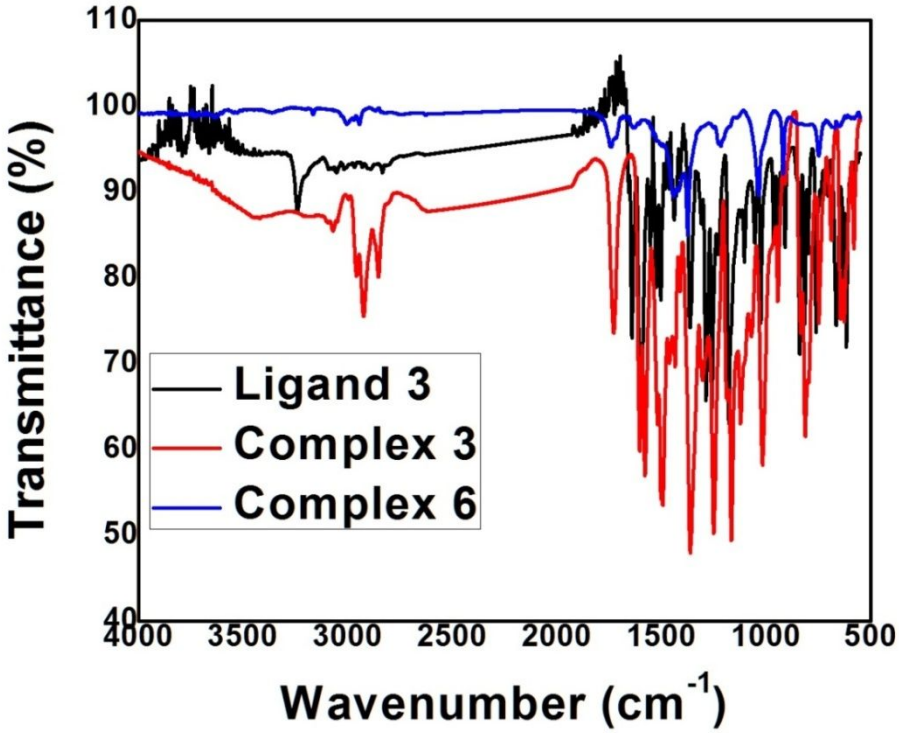

Figure S12. Overlaid FT-IR spectrum of HL3 withcomplex **3** and **6**.

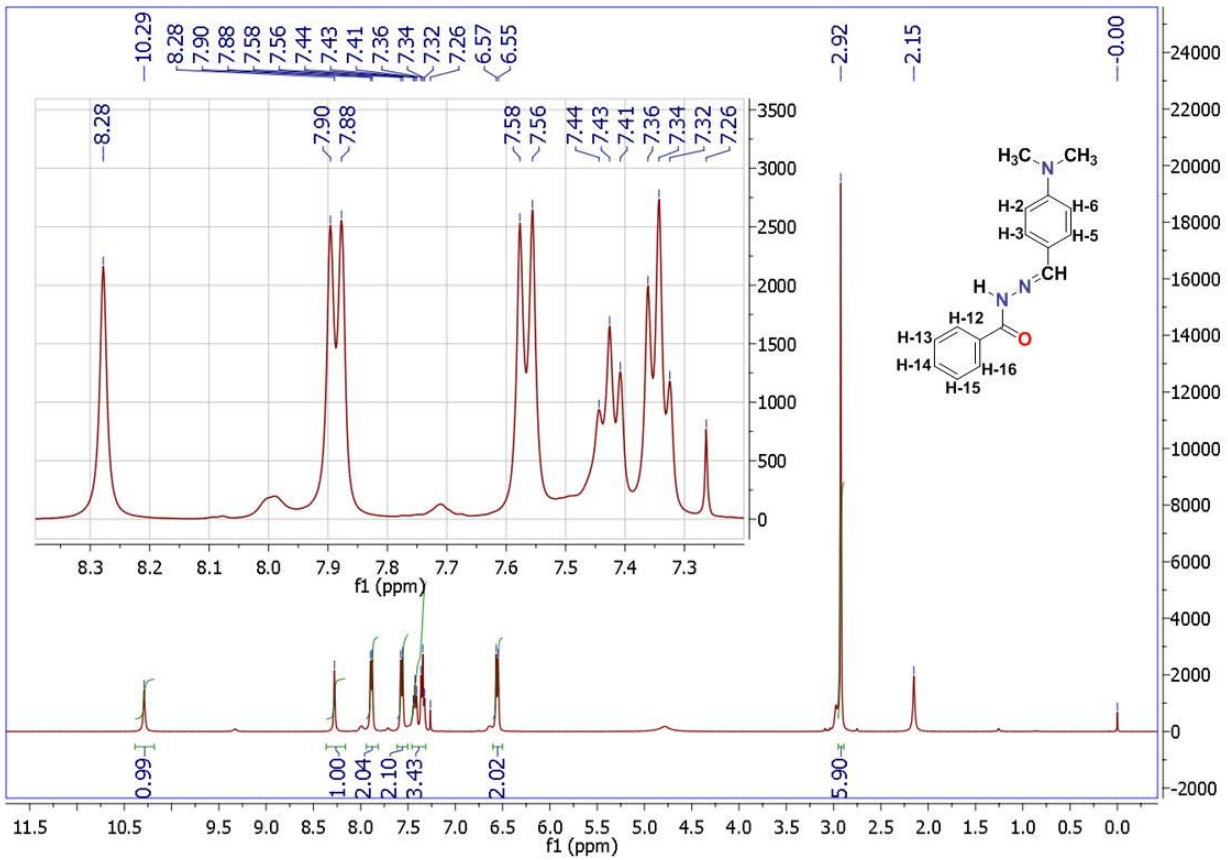

Figure S13. ^{1}H NMR spectrum of HL1 in $CDCl_3$ (400 MHz, 293 K).

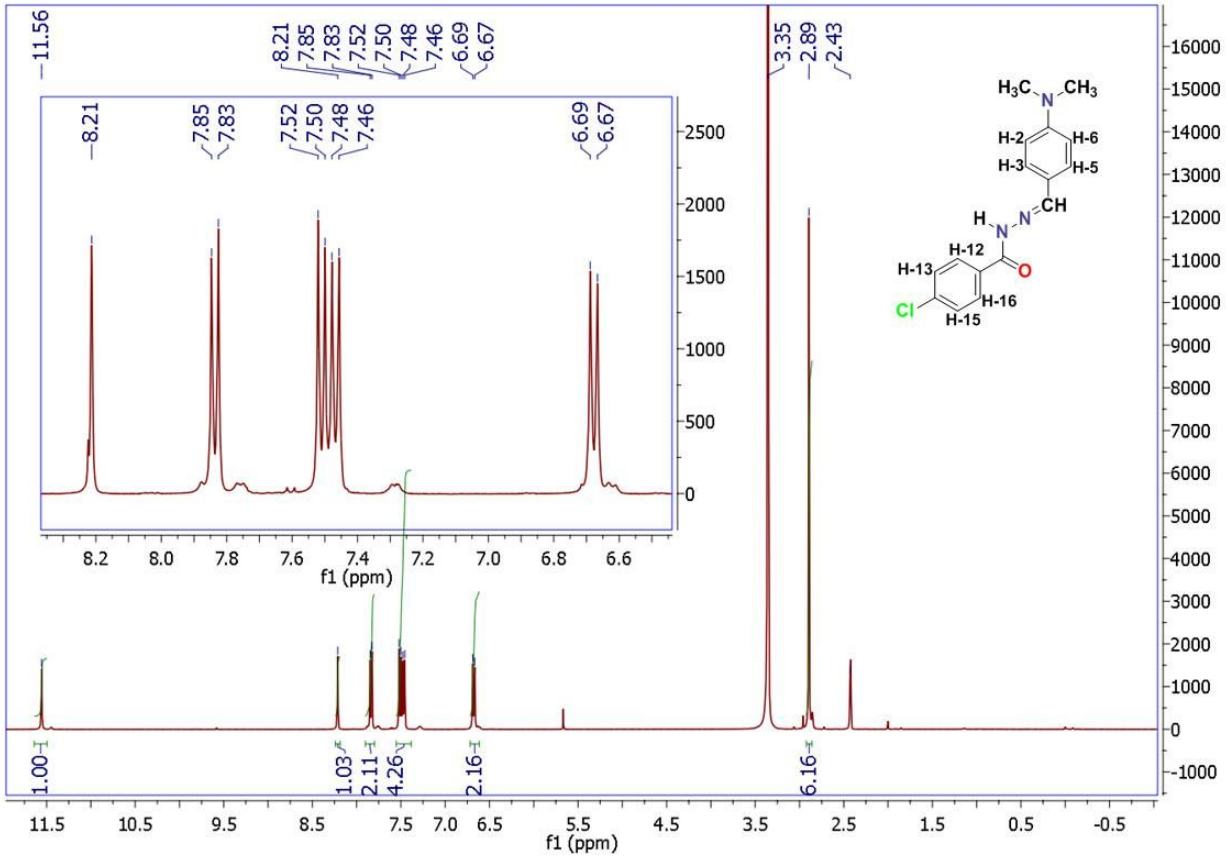

Figure S14. ^{1}H NMR spectrum of HL2 in DMSO-d_6 (400 MHz, 293 K).

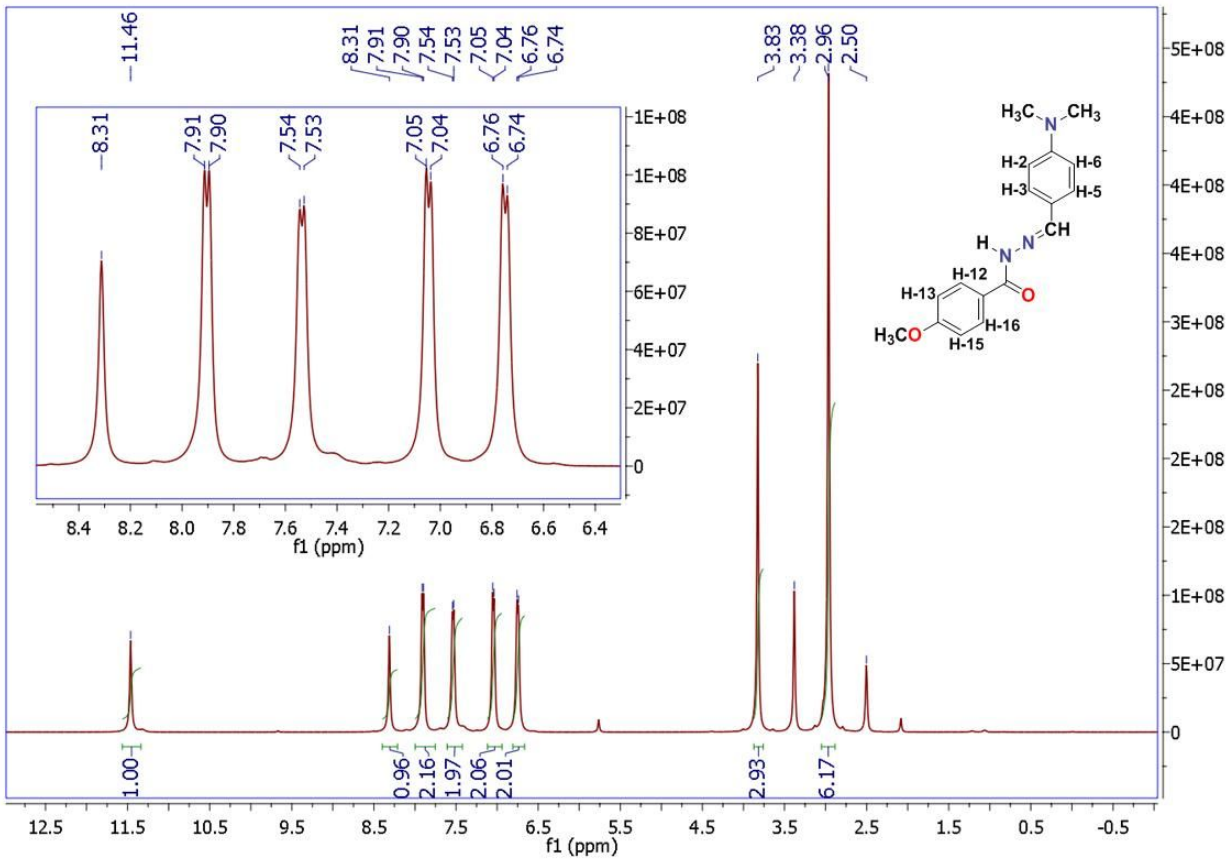

Figure S15. ^{1}H NMR spectrum of HL3 in DMSO-d_6 (400 MHz, 293 K).

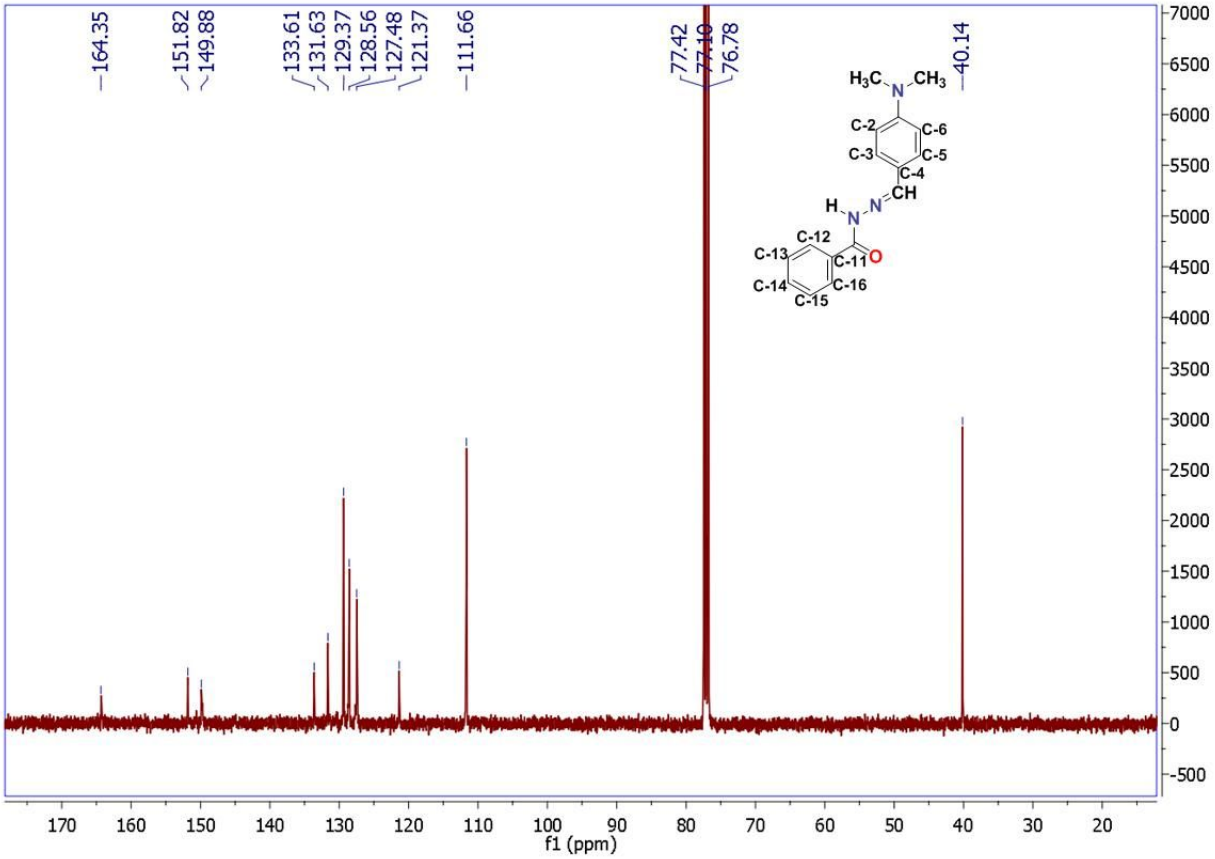

Figure S16. ^{13}C NMR spectrum of HL1 in $CDCl_3$ (100 MHz, 293 K).

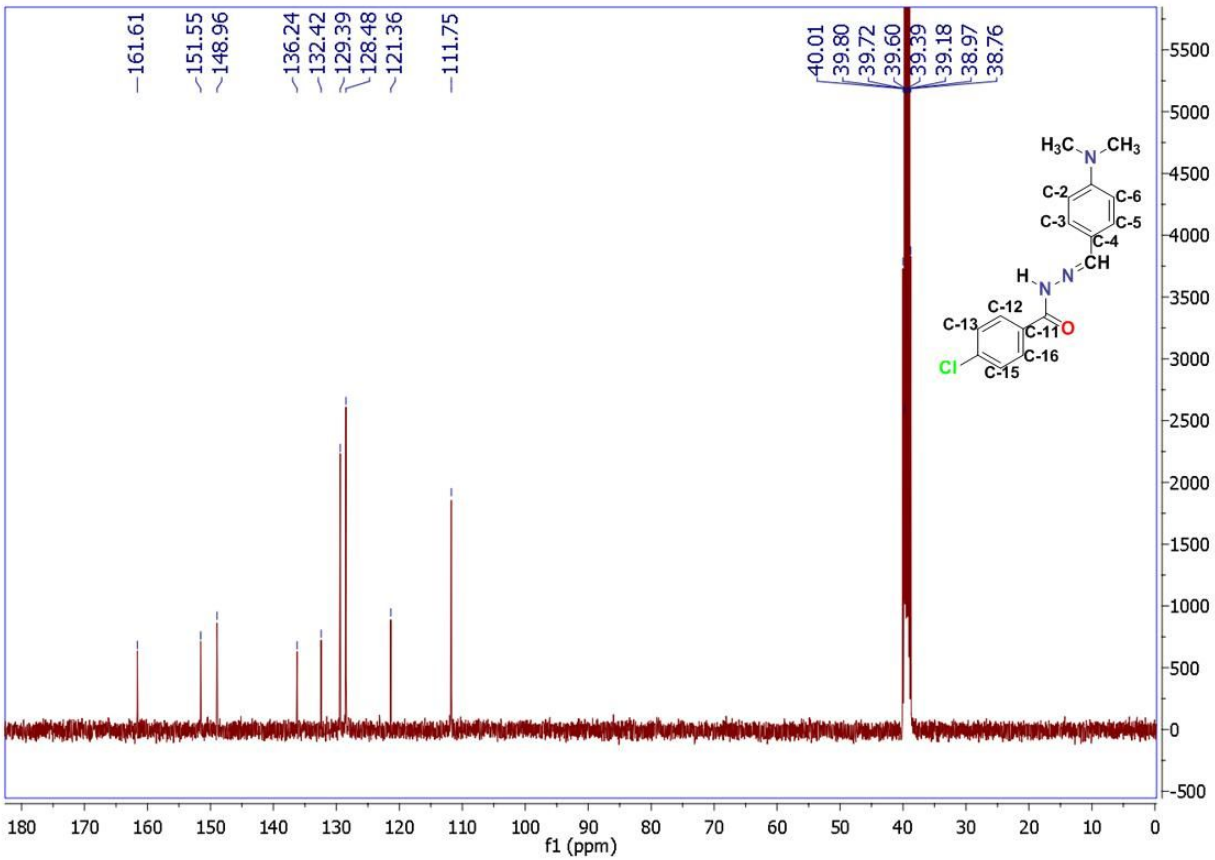

Figure S17. ^{13}C NMR spectrum of HL2 in DMSO-d_6 (100 MHz, 293 K).

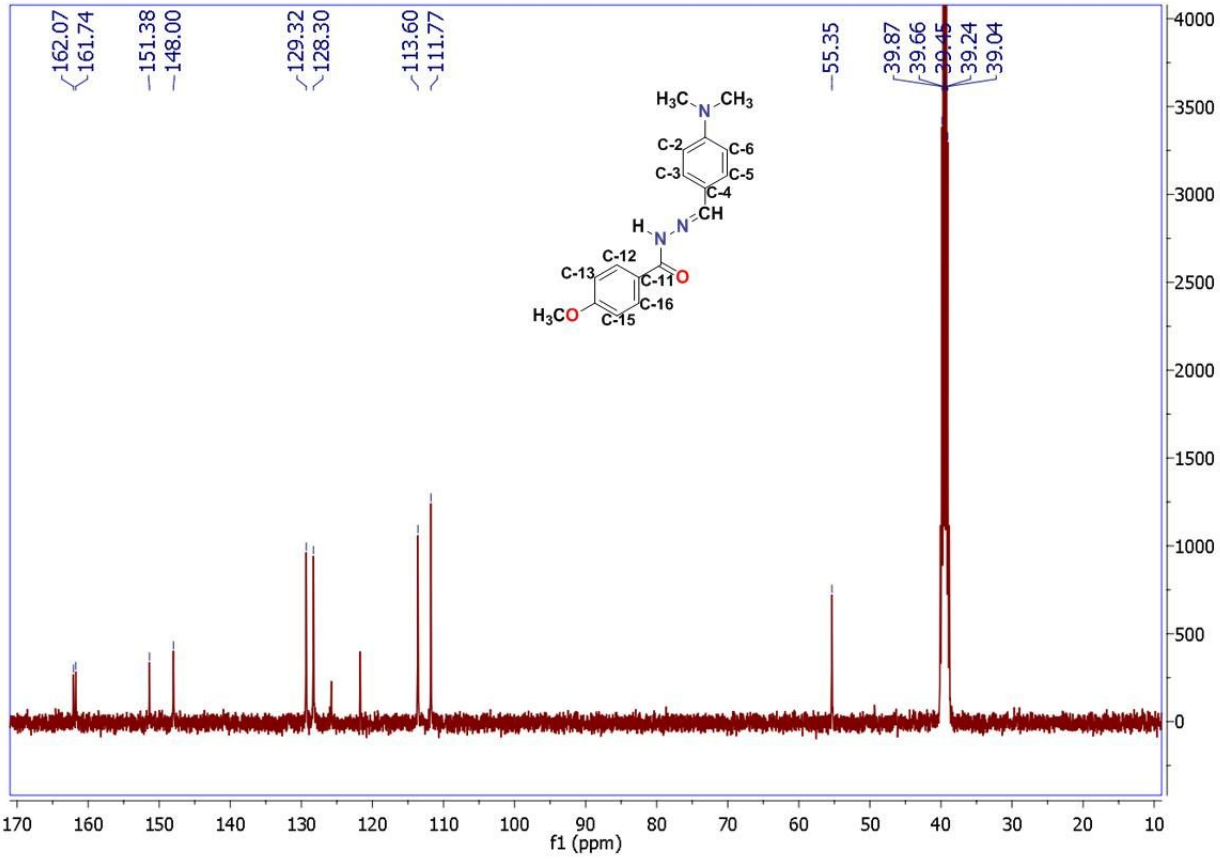

Figure S18. ^{13}C NMR spectrum of HL3 in DMSO-d_6 (100 MHz, 293 K).

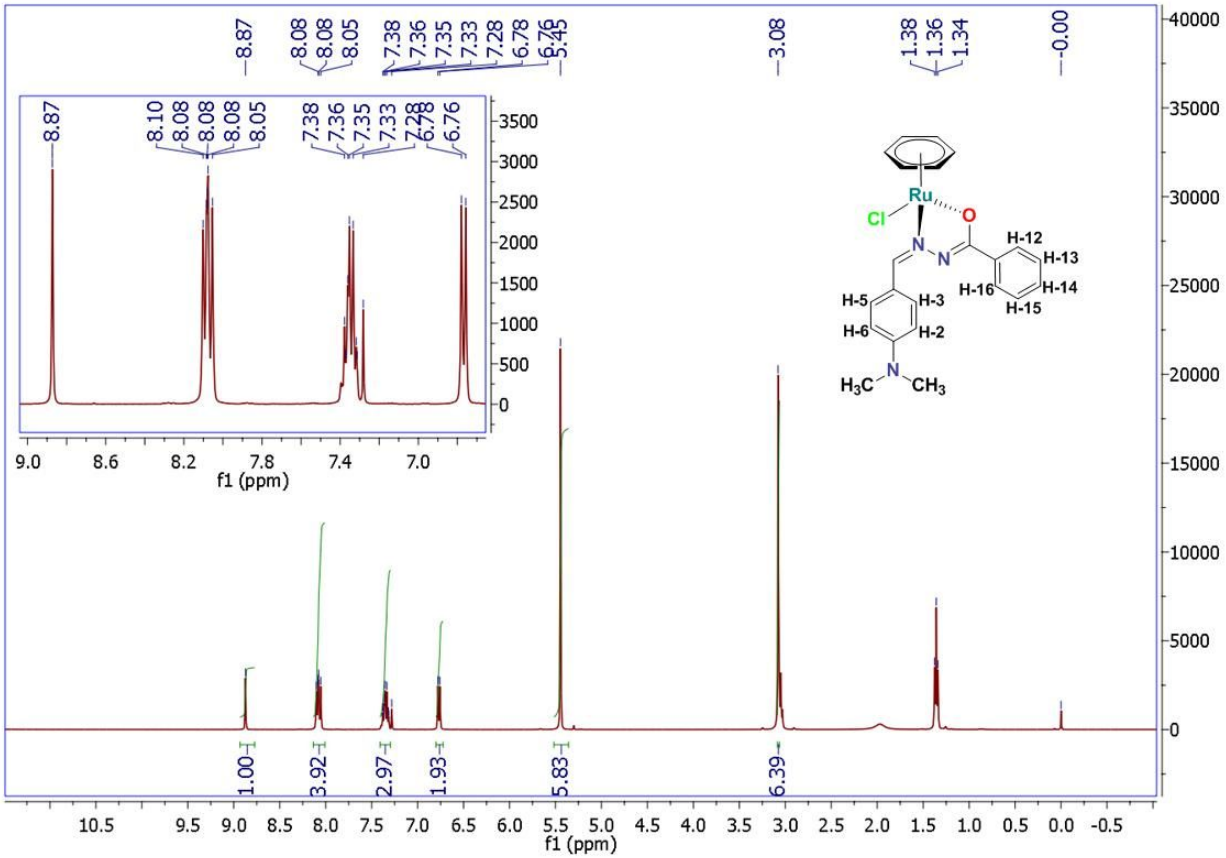

Figure S19. ^{1}H NMR spectrum of [Ru(L1) (η^6-benzene)Cl] (**1**) in $CDCl_3$ (400 MHz, 293 K).

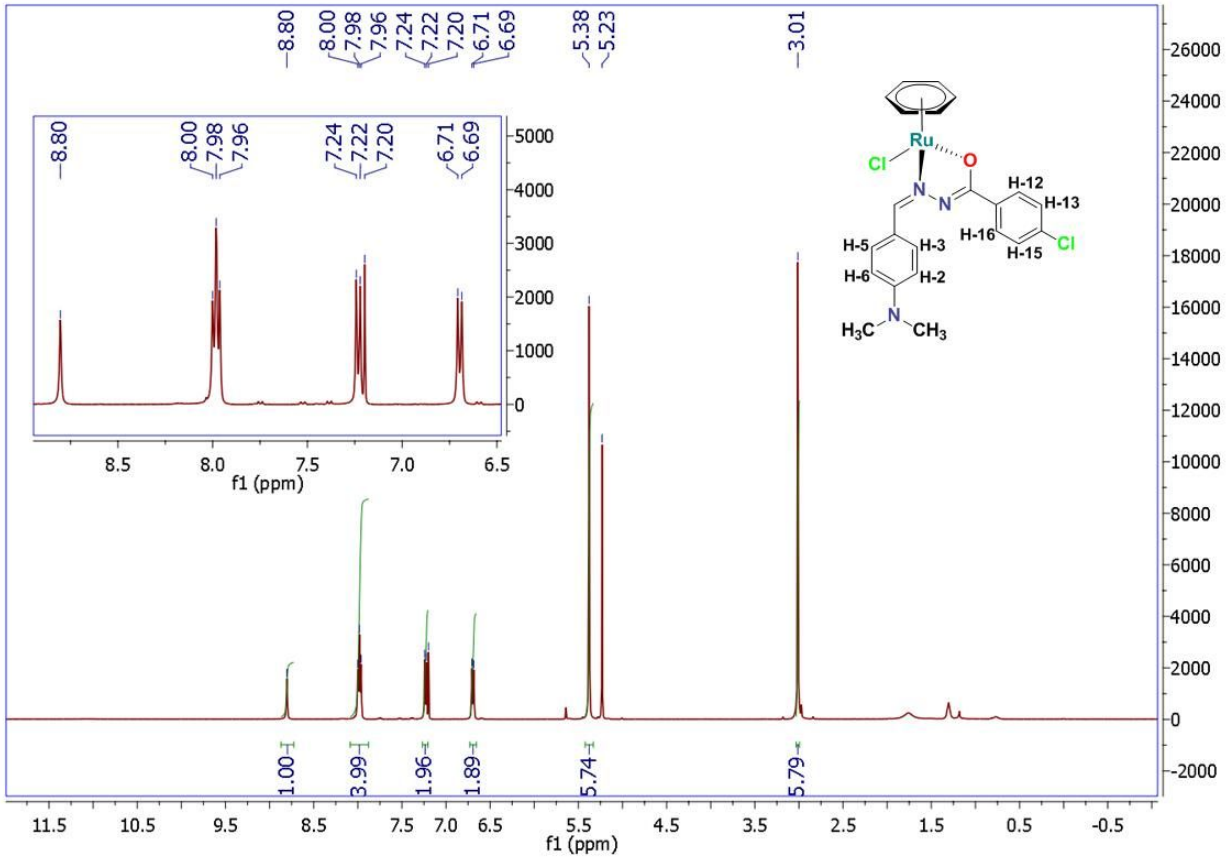

Figure S20. ^{1}H NMR spectrum of [Ru(L2)(η^6-benzene)Cl] **(2)** in $CDCl_3$ (400 MHz, 293 K)**.**

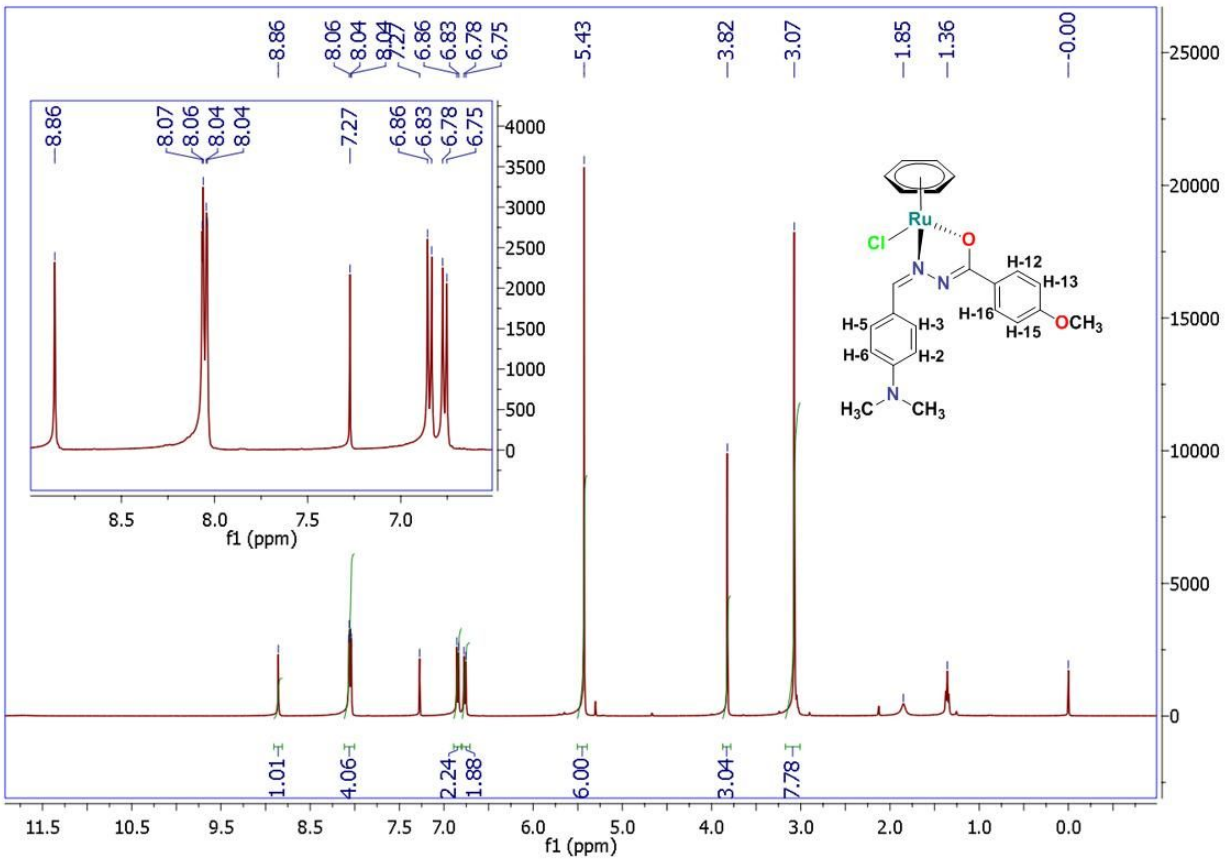

Figure S21. ^{1}H NMR spectrum of [Ru(L3)(η^{6}-benzene)Cl] **(3)** in $CDCl_3$ (400 MHz, 293 K)**.**

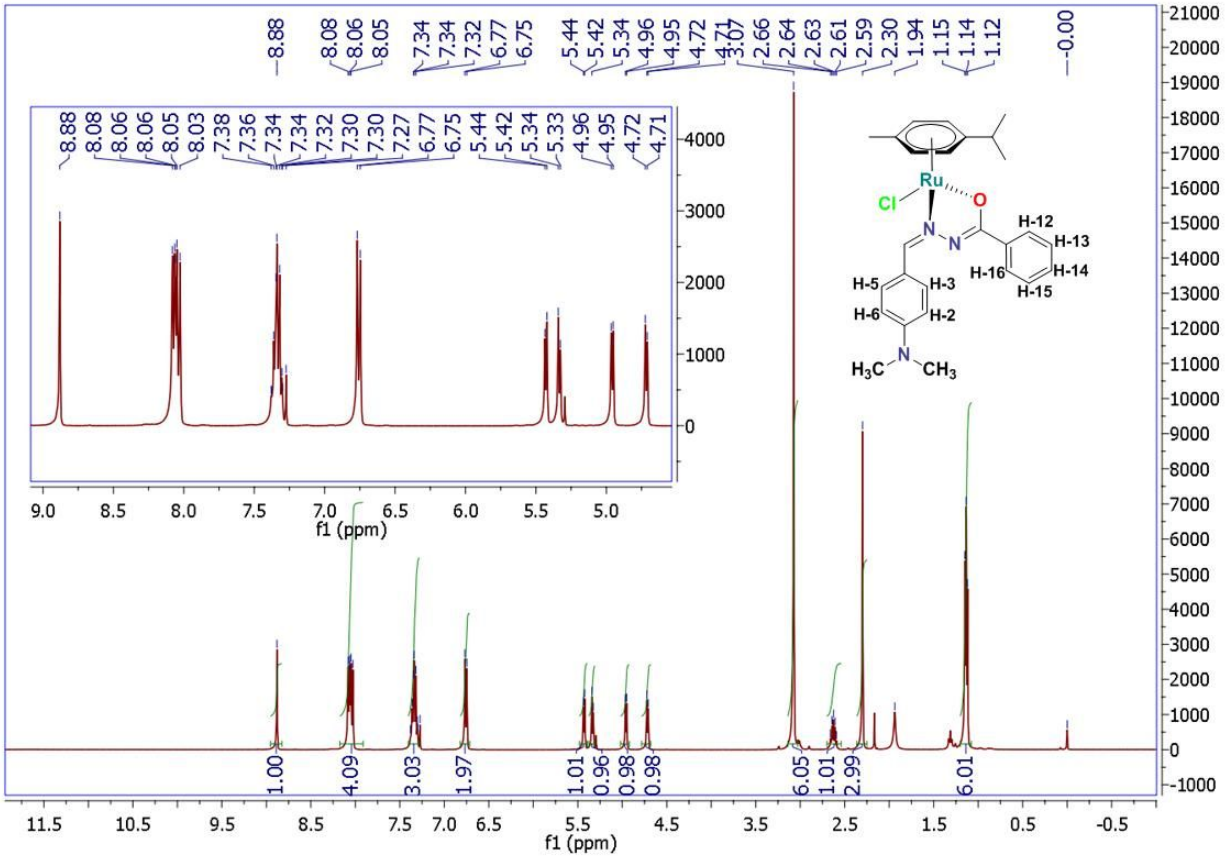

Figure S22. ^{1}H NMR spectrum of [Ru(L1)(η^{6}-*p*-cymene)Cl] **(4)** in $CDCl_3$ (400 MHz, 293 K)**.**

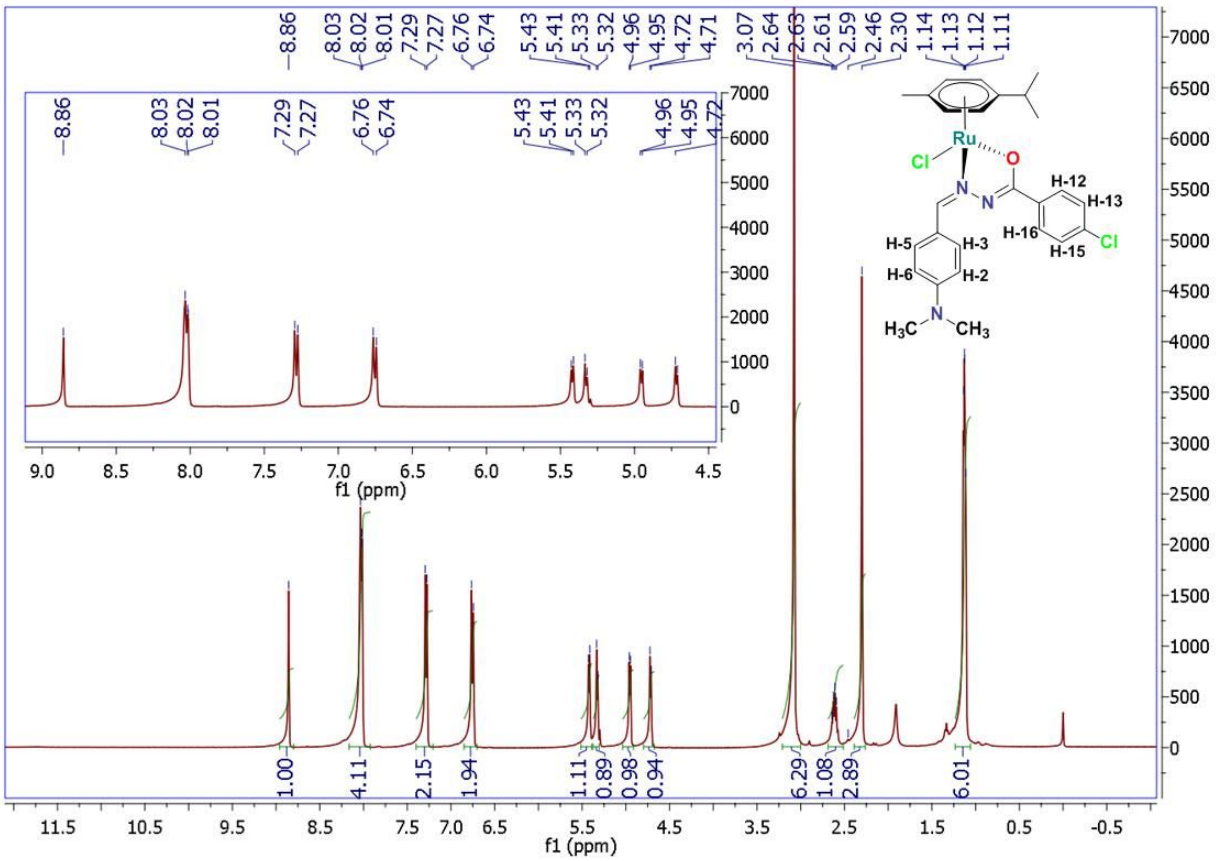

Figure S23. ^{1}H NMR spectrum of [Ru(L2)(η^{6}-*p*-cymene)Cl] **(5)** in $CDCl_3$ (400 MHz, 293 K)**.**

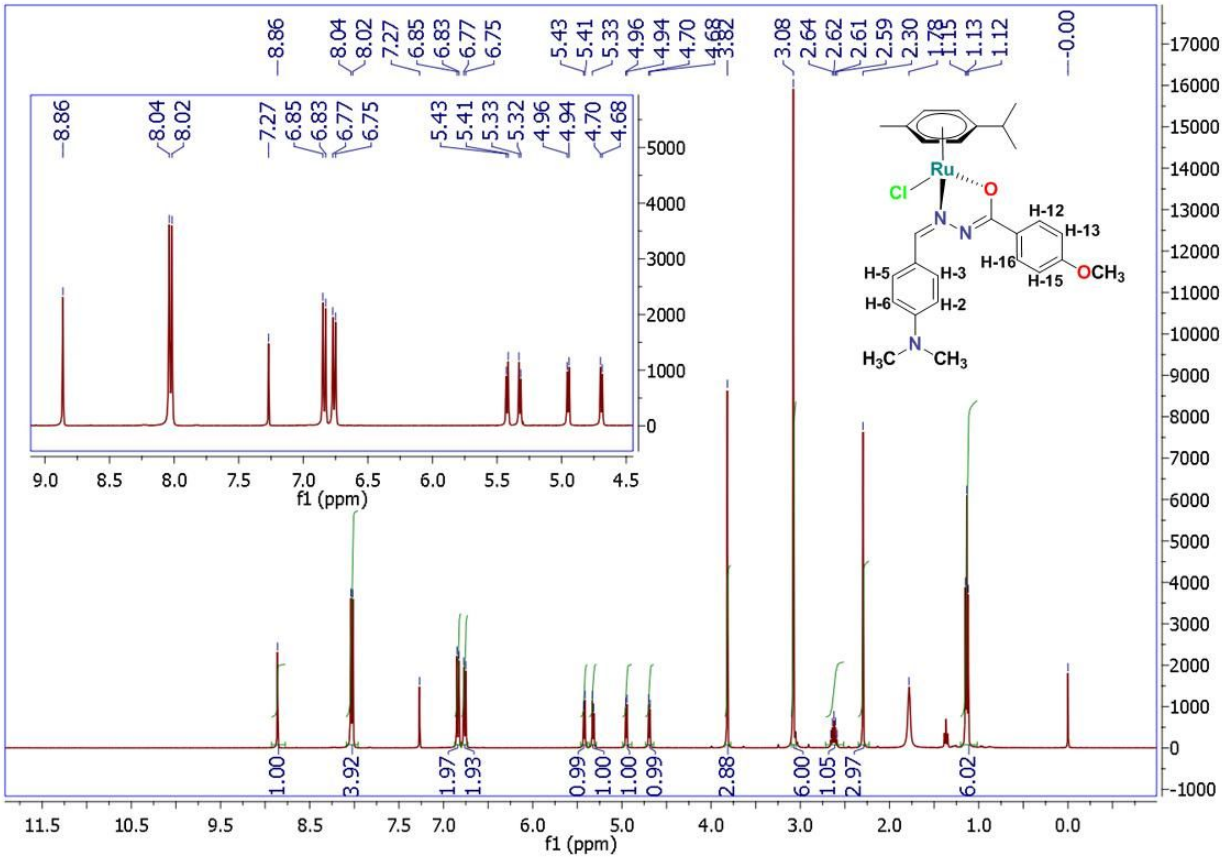

Figure S24. ^{1}H NMR spectrum of [Ru(L3)(η^{6}-*p*-cymene)Cl] **(6)** in $CDCl_3$ (400 MHz, 293 K)**.**

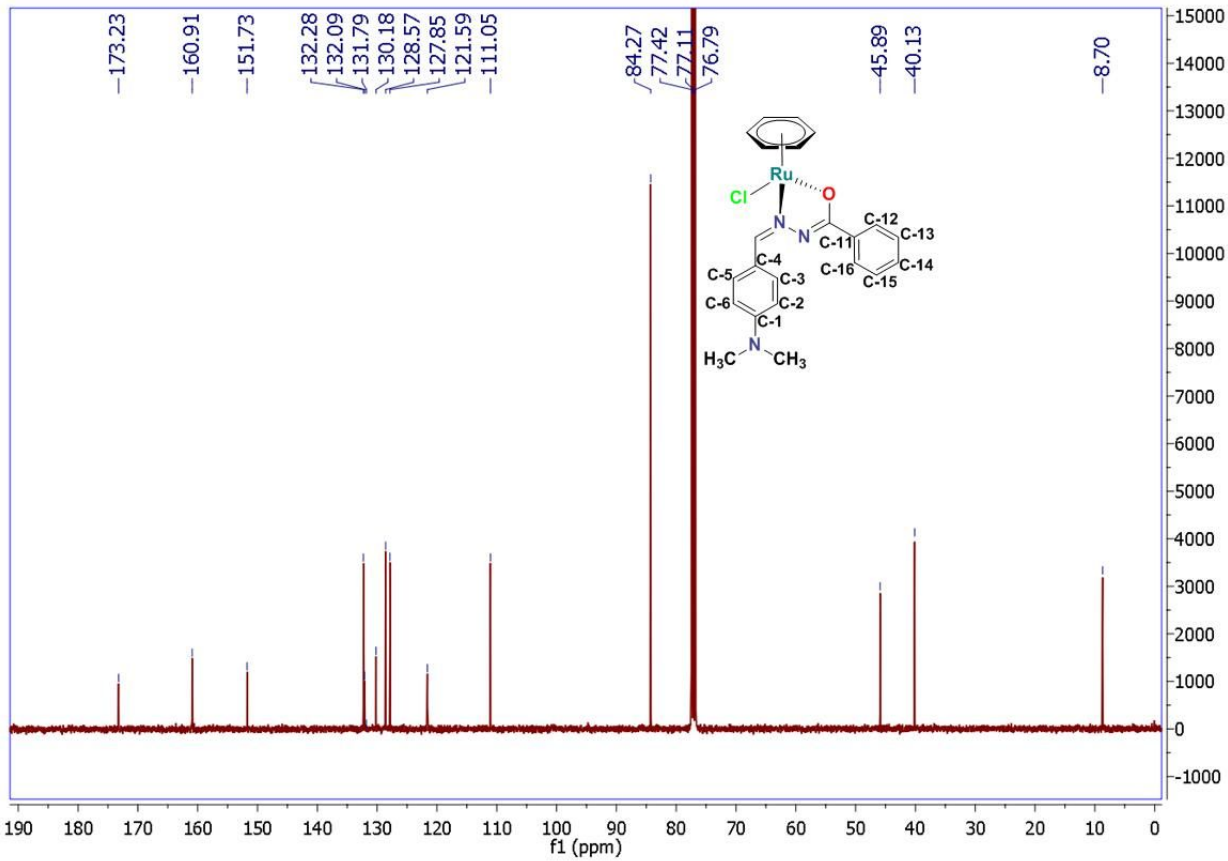

Figure S25. ^{13}C NMR spectrum of [Ru(L1) (η^6-benzene)Cl] **(1)** in $CDCl_3$ (100 MHz, 293 K).

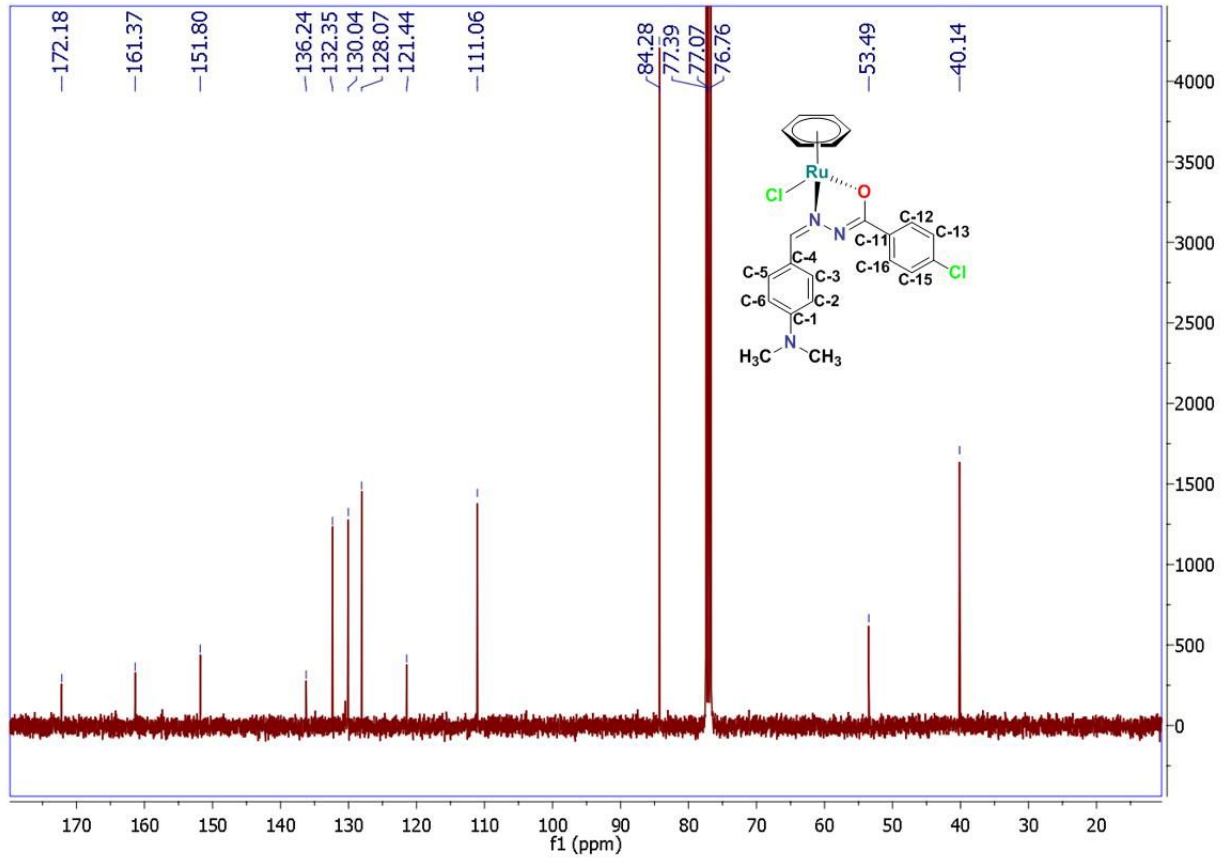

Figure S26. ^{13}C NMR spectrum of [Ru(L2)(η^6-benzene)Cl] **(2)** in $CDCl_3$ (100 MHz, 293 K).

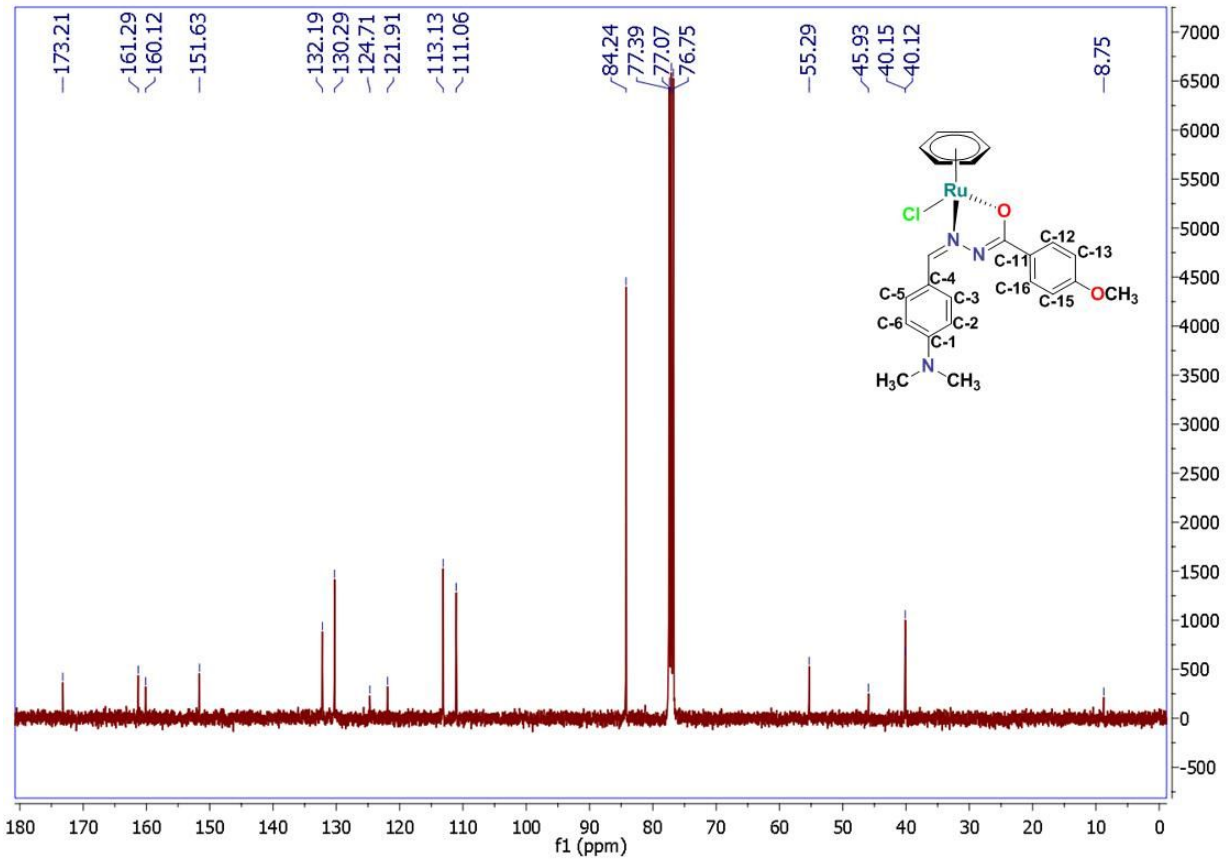

Figure S27. ^{13}C NMR spectrum of [Ru(L3)(η^6-benzene)Cl] **(3)** in $CDCl_3$ (100 MHz, 293 K)**.**

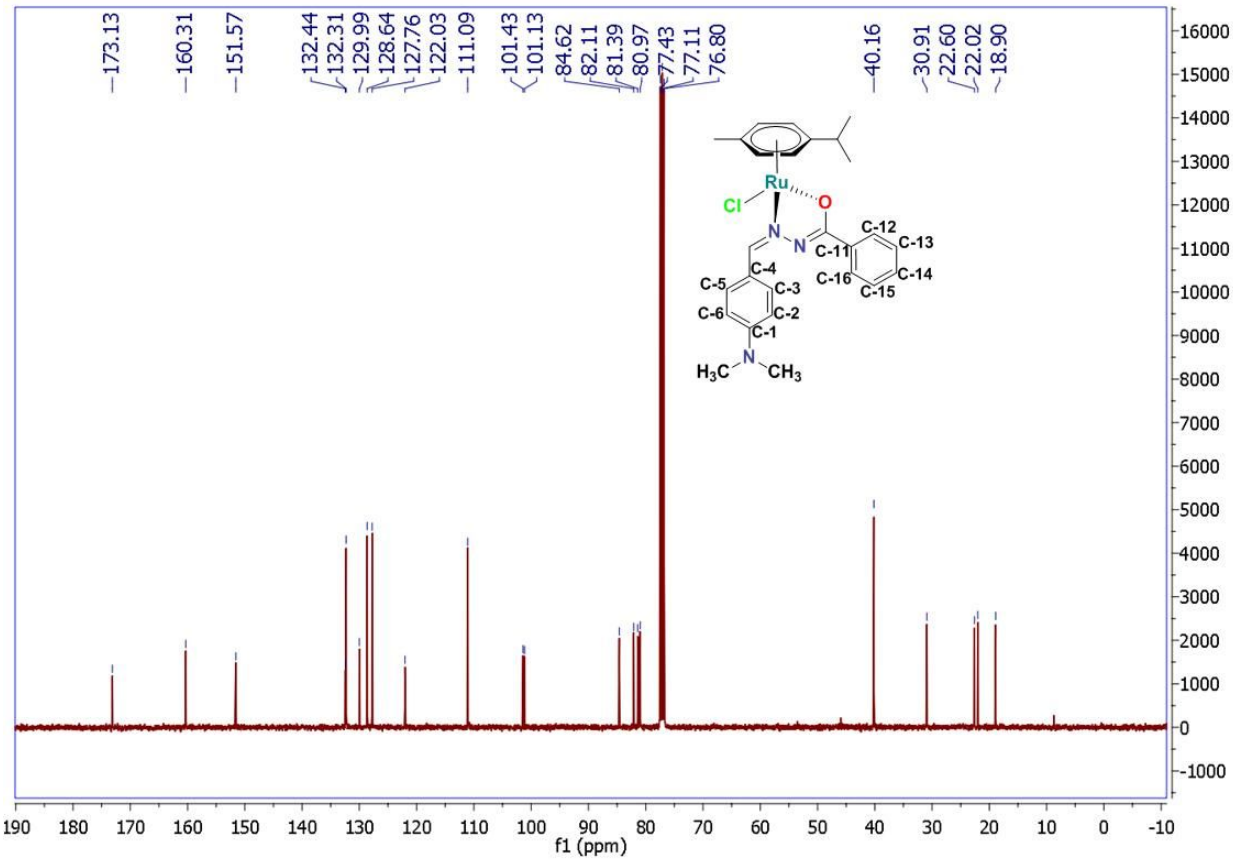

Figure S28.^{13}C NMR spectrum of [Ru(L1)(η^6-*p*-cymene)Cl] **(4)** in $CDCl_3$ (100 MHz, 293 K)**.**

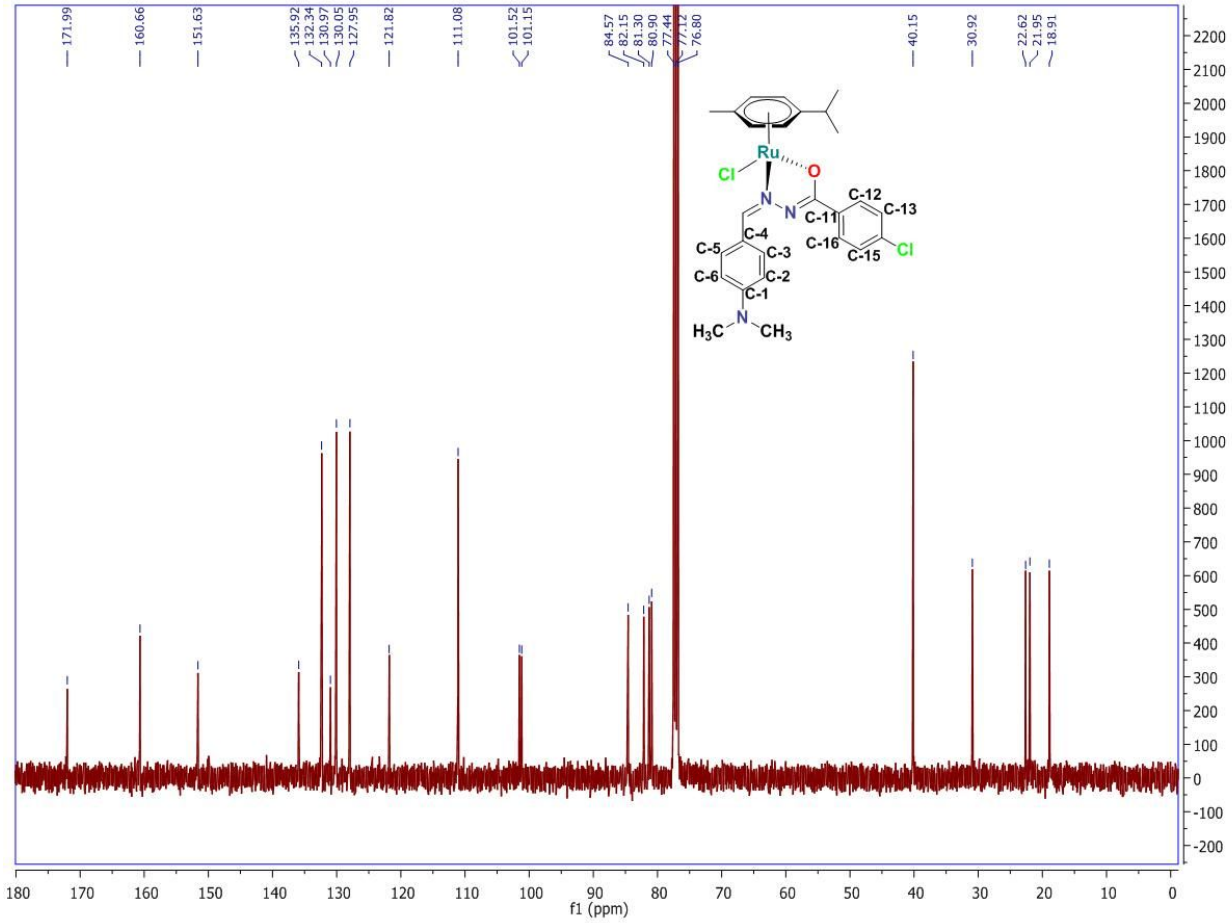

Figure S29. ^{13}C NMR spectrum of [Ru(L2)(η^6-*p*-cymene)Cl]**(5)** in $CDCl_3$(100 MHz, 293 K)**.**

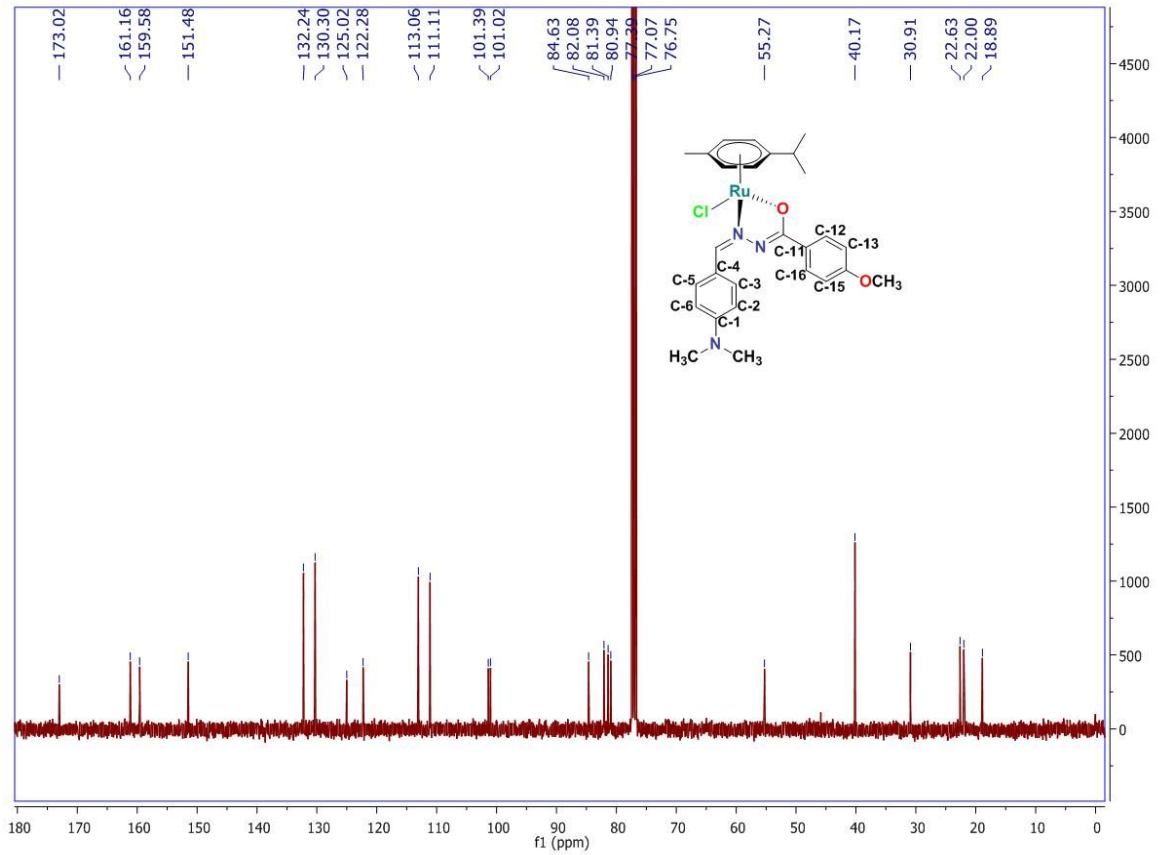

Figure S30. ^{13}C NMR spectrum of [Ru(L3)(η^6-*p*-cymene)Cl] **(6)** in $CDCl_3$(100 MHz, 293 K).

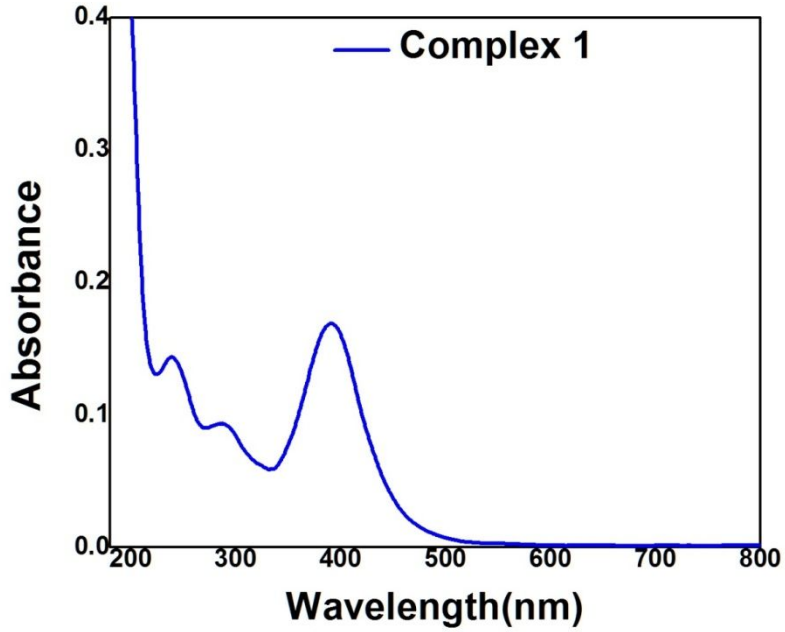

Figure S31. UV-Vis spectrum of complex **1** [A_{max} (nm): 383, 292, 230].

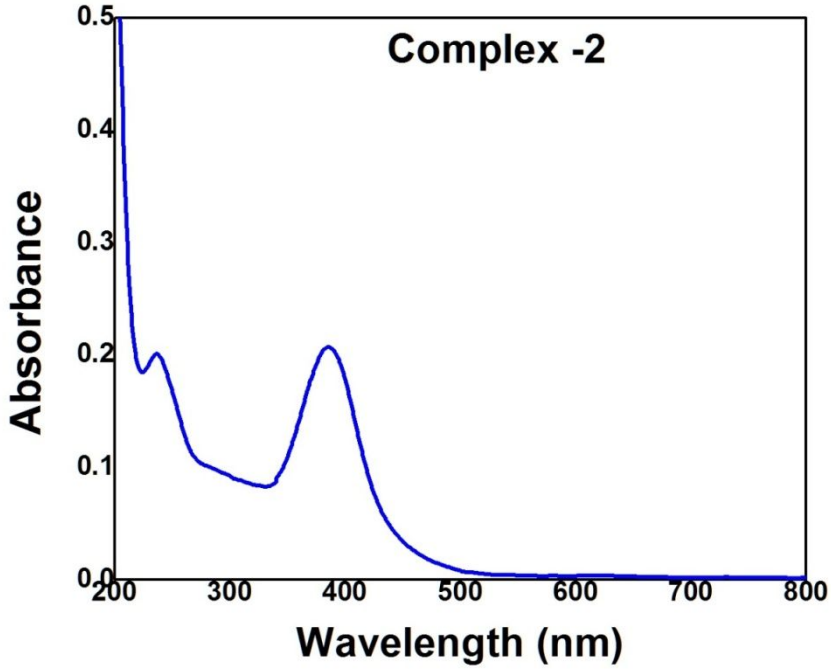

Figure S32. UV-Vis spectrum of complex **2** [A_{max} (nm): 389, 291, 233].

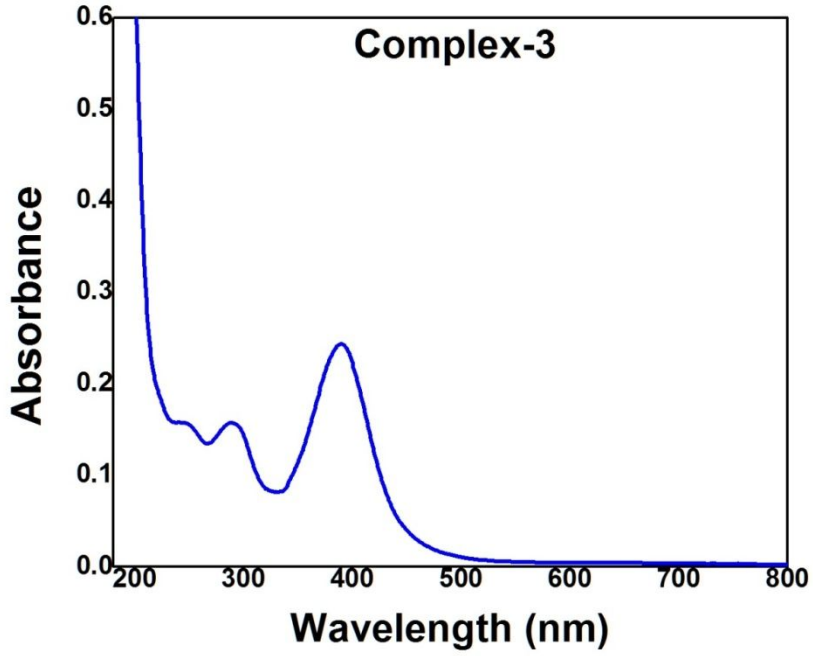

Figure S33.UV-Vis spectrum of complex **3** [A_{max} (nm): 387, 293, 233].

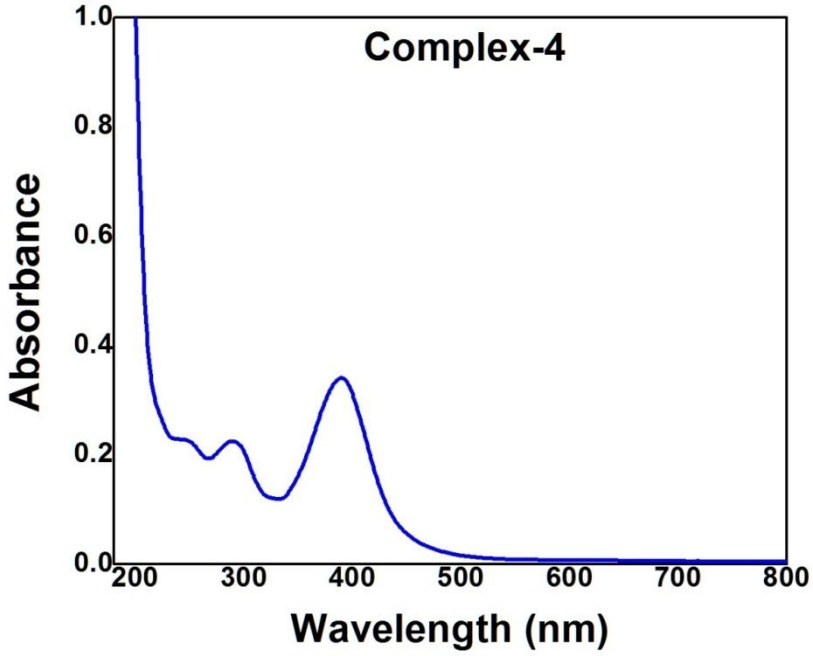

Figure S34. UV-Vis spectrum of complex **4** [A_{max} (nm): 387, 294, 231].

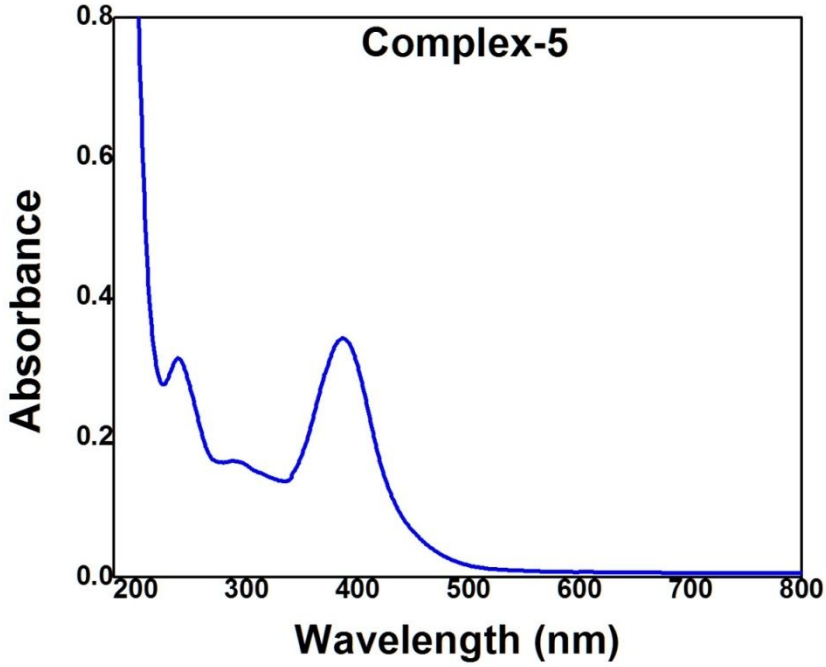

Figure S35. UV-Vis spectrum of complex **5** [A_{max} (nm): 388, 287, 236].

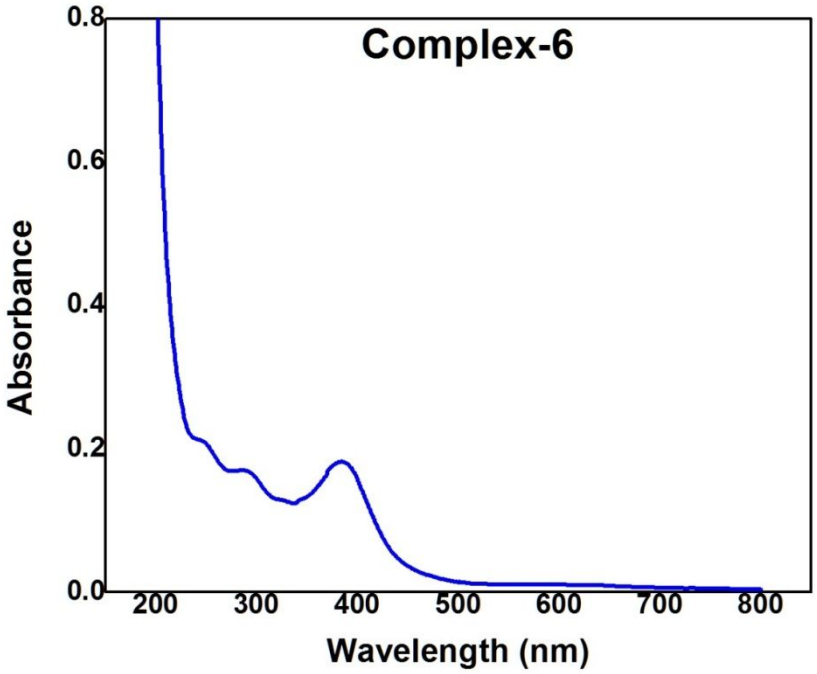

Figure S36. UV-Vis spectrum of complex 6 [A_{max}, nm: 385, 290, 234].

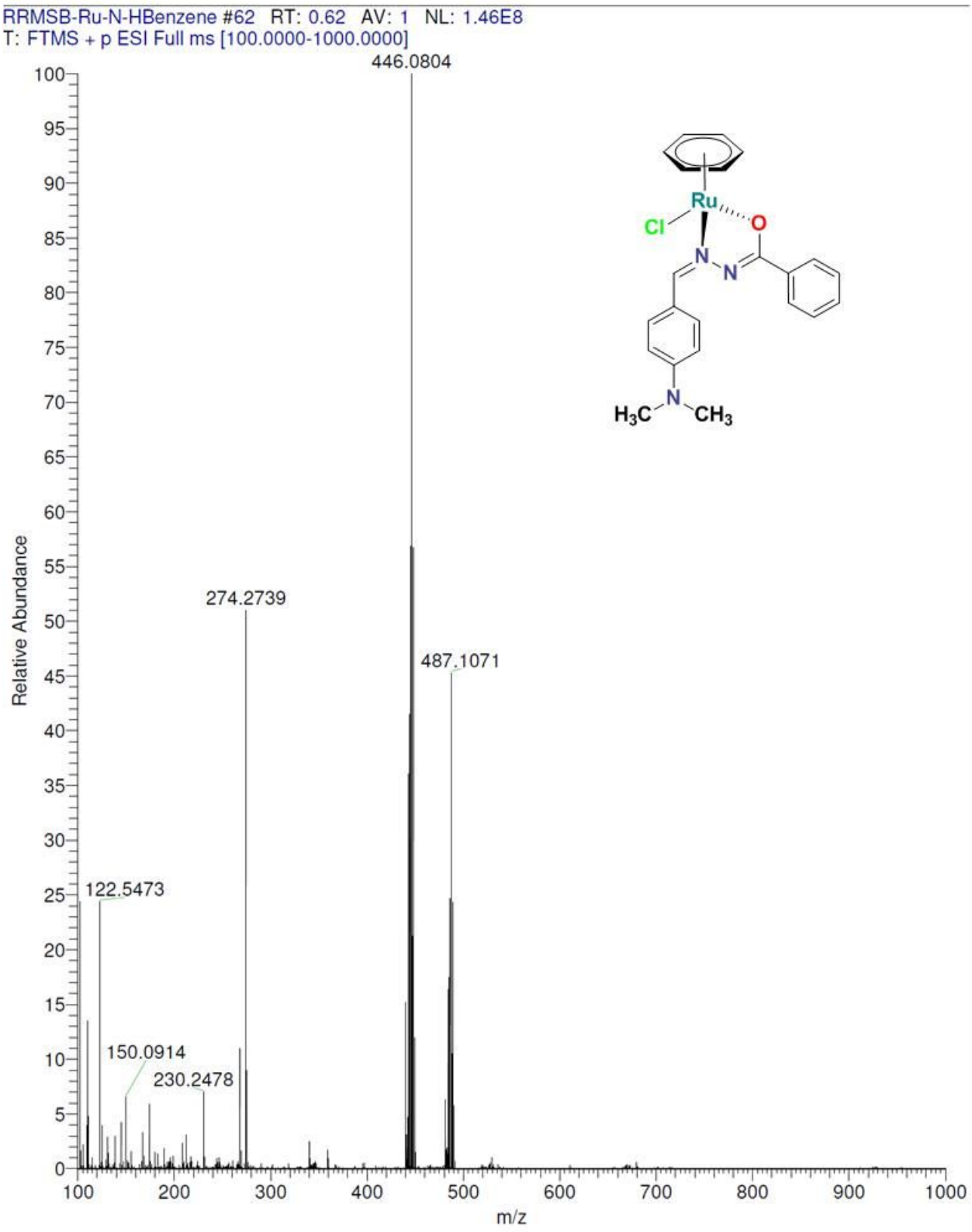

Figure S37. ESI-MS spectrum of [Ru(L1)(η^6-benzene)Cl] **(1)** in acetonitrile; m/z: 446.10$[M\text{-}Cl]^+$.

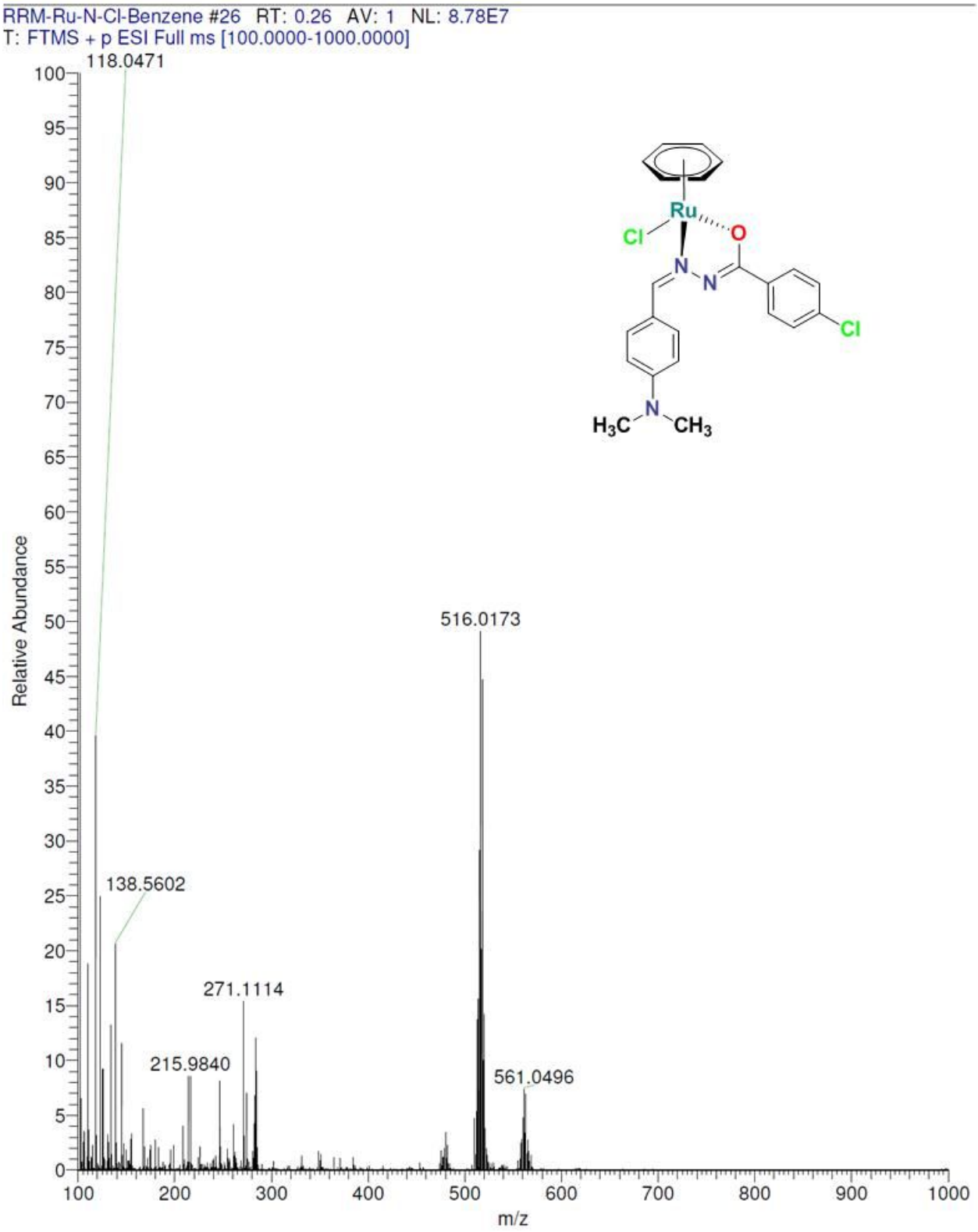

Figure S38. ESI-MS spectrum of [Ru(L2)(η^6-benzene)Cl] **(2)** in acetonitrile; m/z: 516.0$[M+H]^+$.

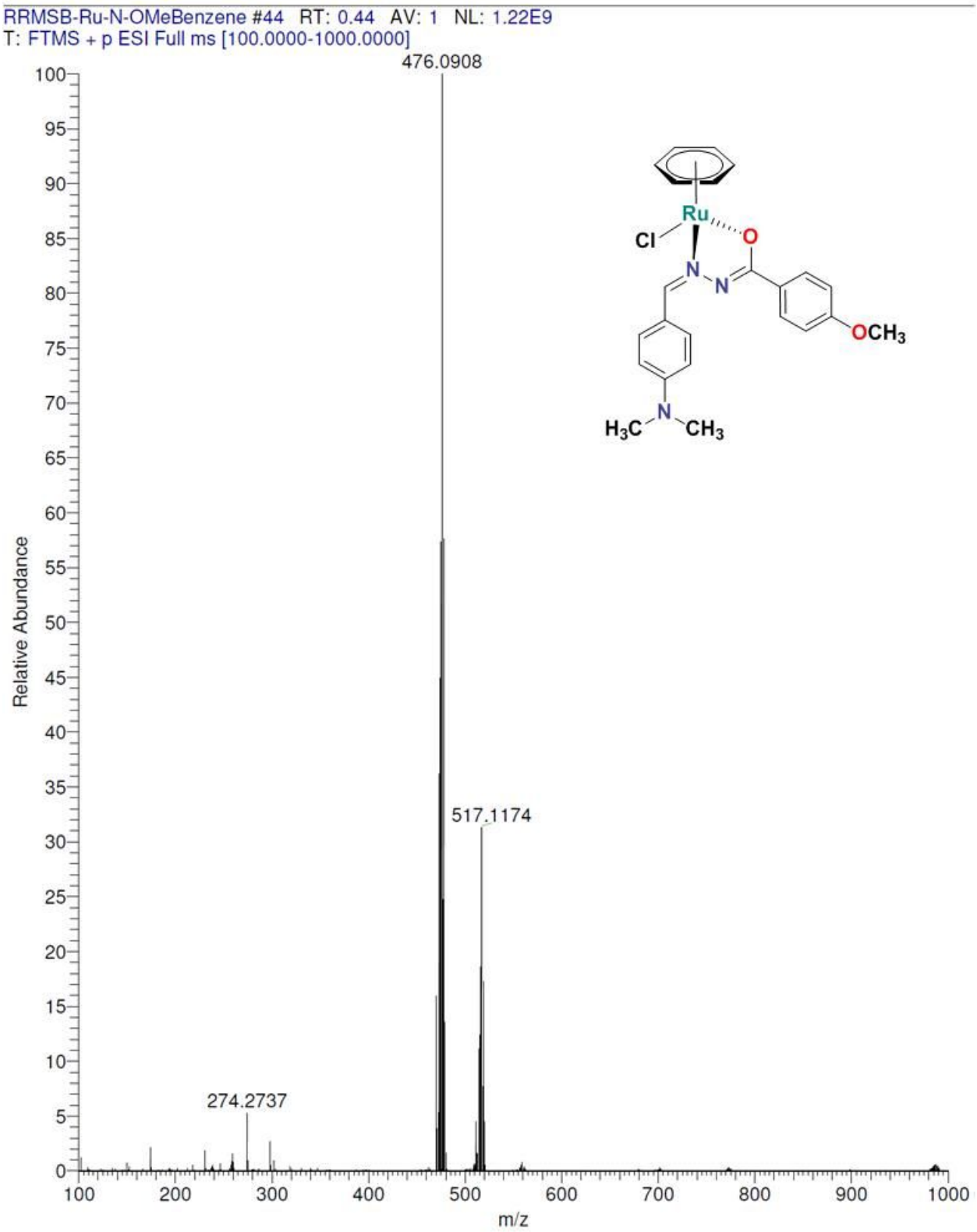

Figure S39. ESI-MS spectrum of [Ru(L3)(η^6-benzene)Cl] **(3)** in acetonitrile; m/z: 476.10$[M\text{-}Cl]^+$.

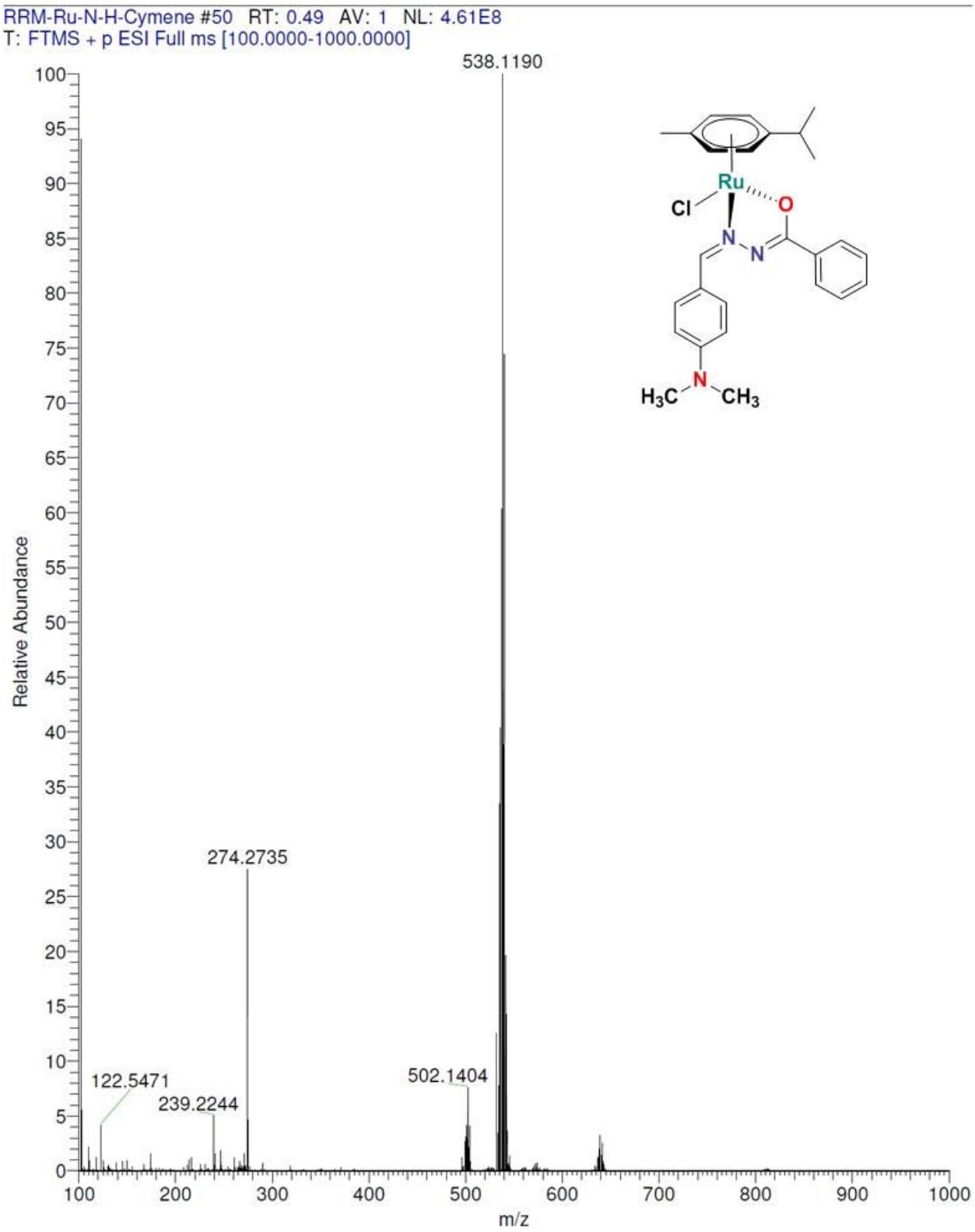

Figure S40. ESI-MS spectrum of [Ru(L1)(η^6-*p*-cymene)Cl] **(4)** in acetonitrile; m/z: 538.10 $[M+H]^+$.

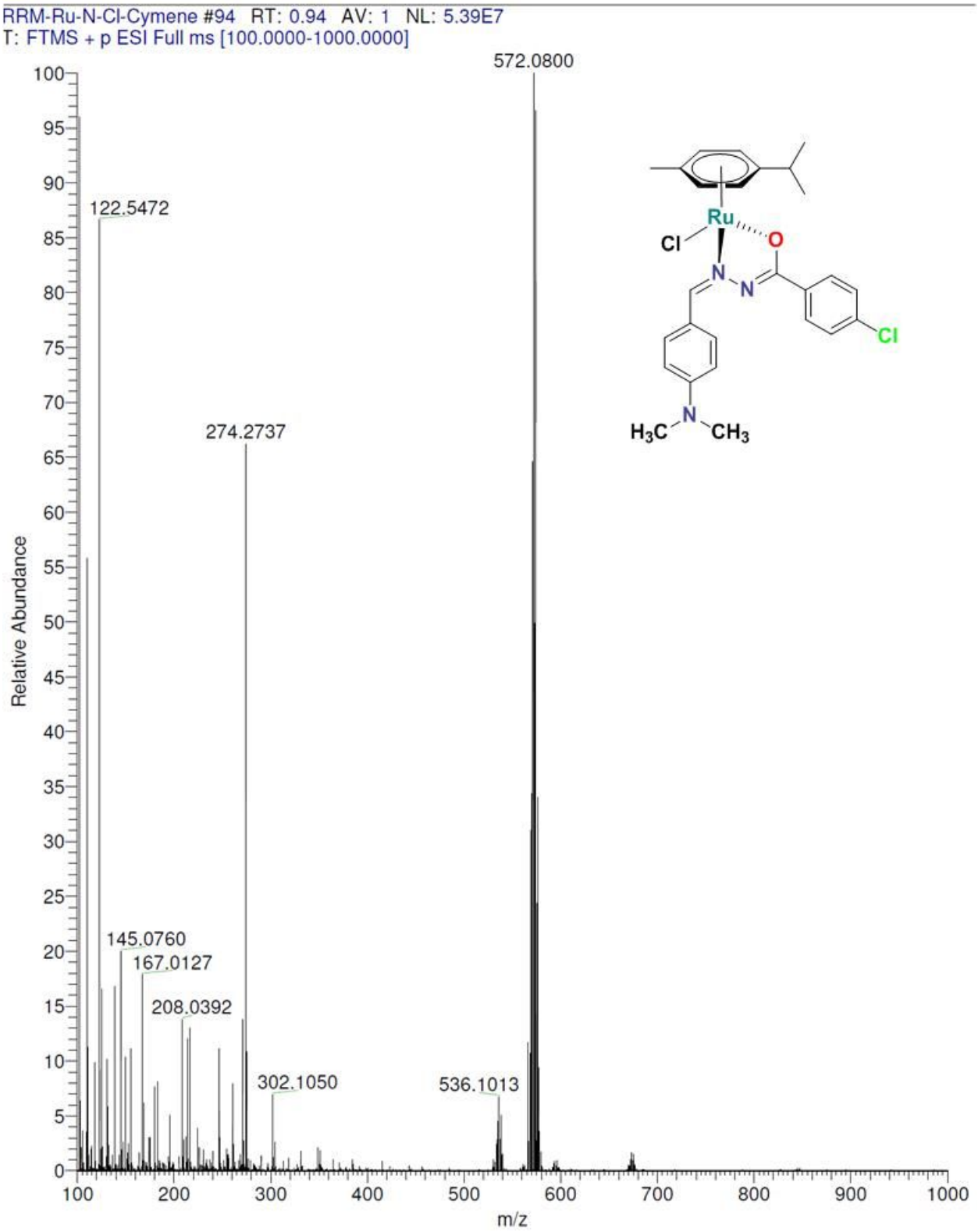

Figure S41. ESI-MS spectrum of [Ru(L2)(η^6-*p*-cymene)Cl] **(5)** in acetonitrile; m/z: 572.10 $[M+H]^+$.

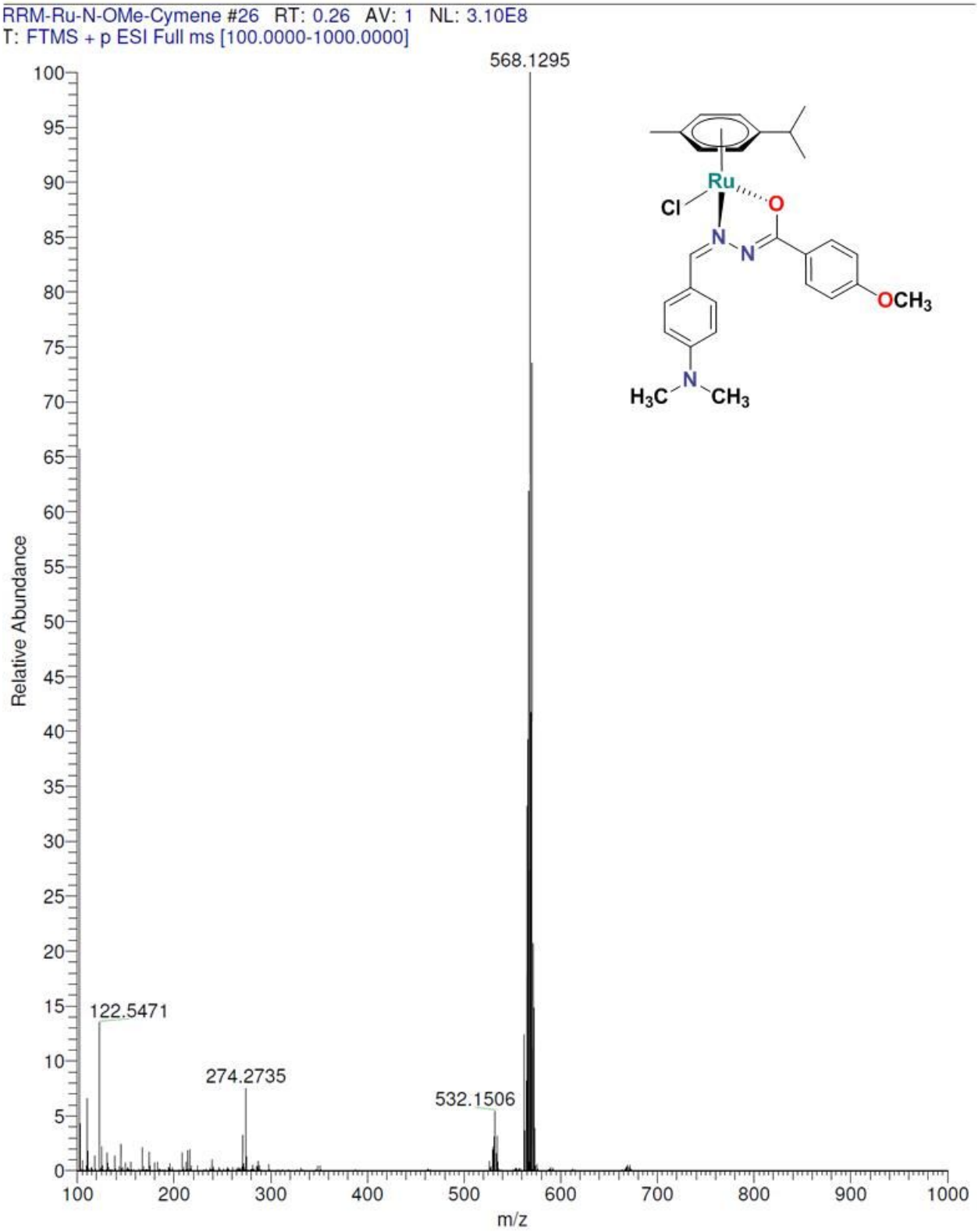

Figure S42. ESI-MS spectrum of [Ru(L3)(η^6-*p*-cymene)Cl] **(6)** in acetonitrile; m/z: 568.12 $[M+H]^+$.

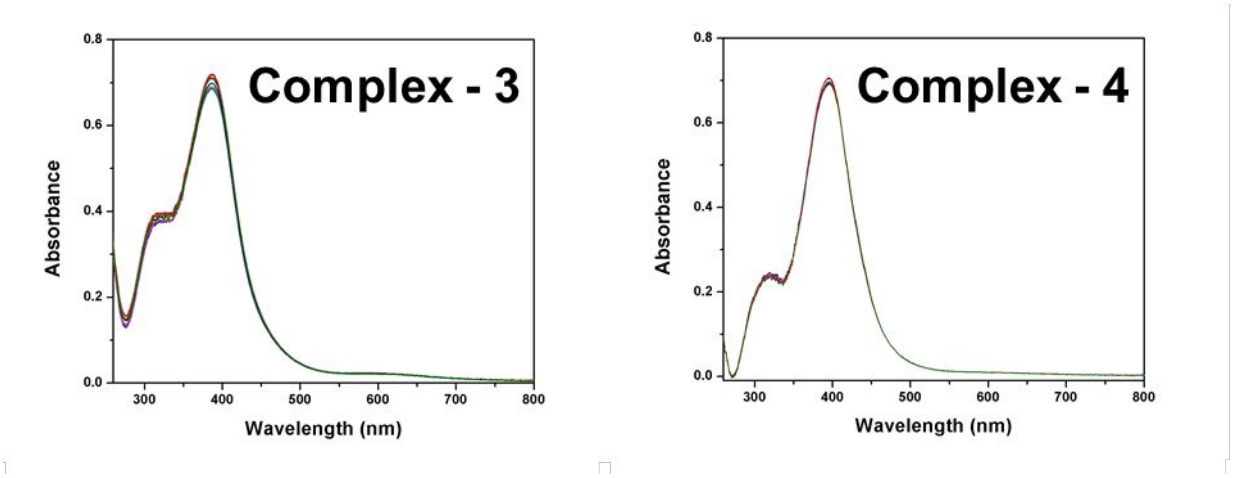

Figure S43. Stability studies of the representative complexes **3** and **4** in 1% DMSO in PBS solution at various time intervals.

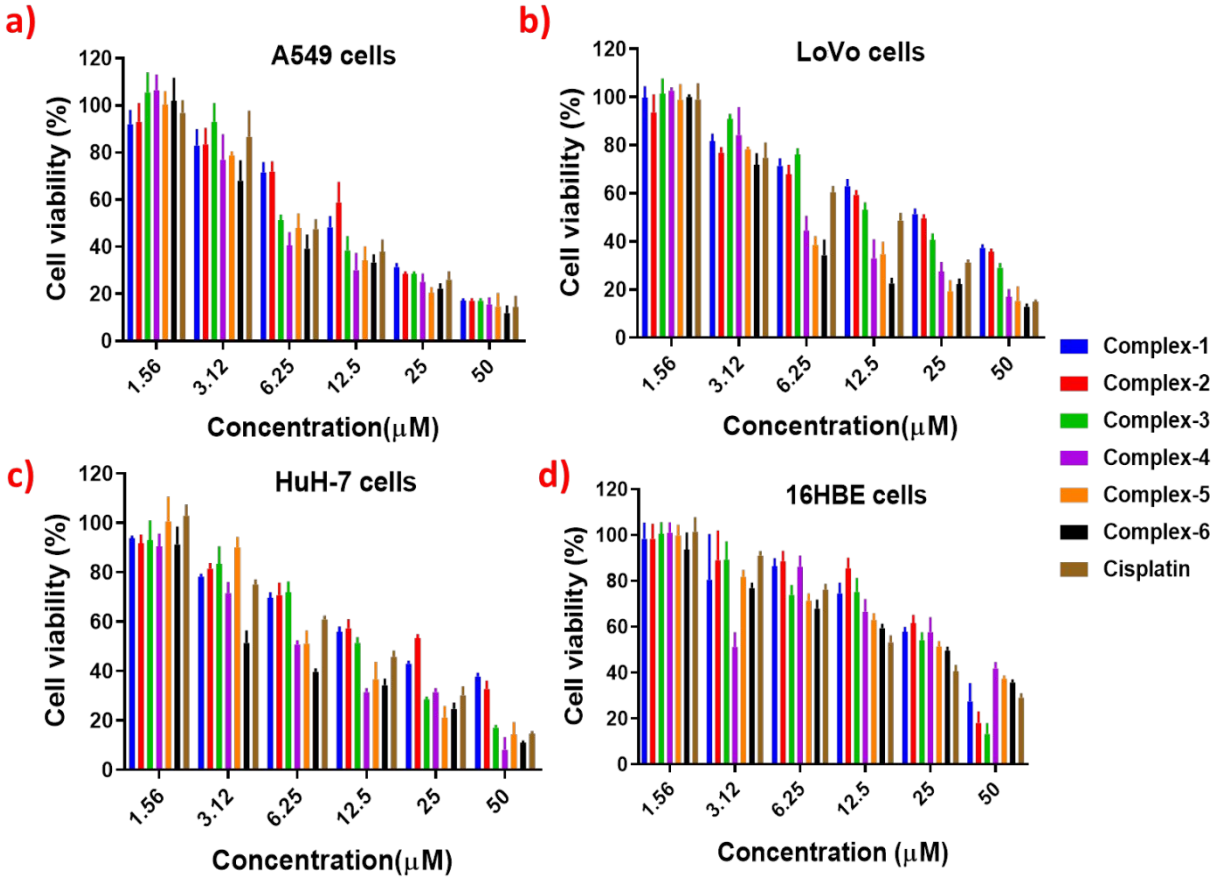

Figure S44. *In vitro cytotoxicity* in (a) A549 cells, (b) LoVo cells (c) HuH-7 cells and (d) 16HBE cells after 72 h of treatment with complexes **1-6** and Cisplatin.

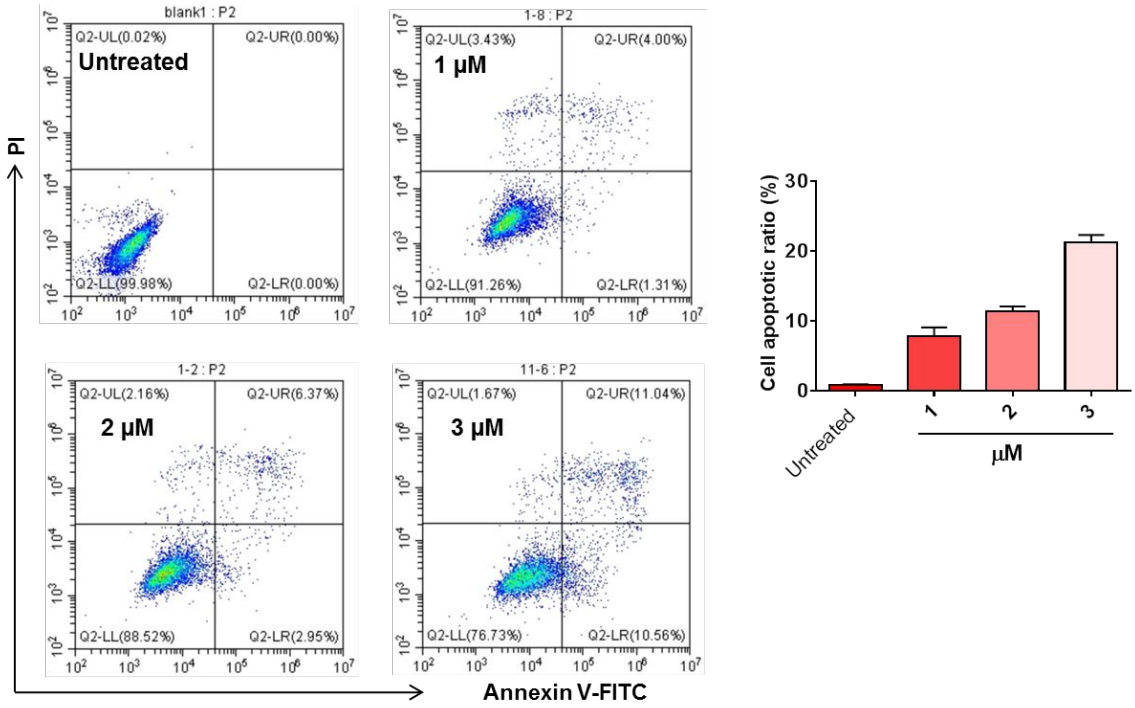

Figure S45. Dose dependent activity of complex **6** in inducing apoptosis by flow cytometry.

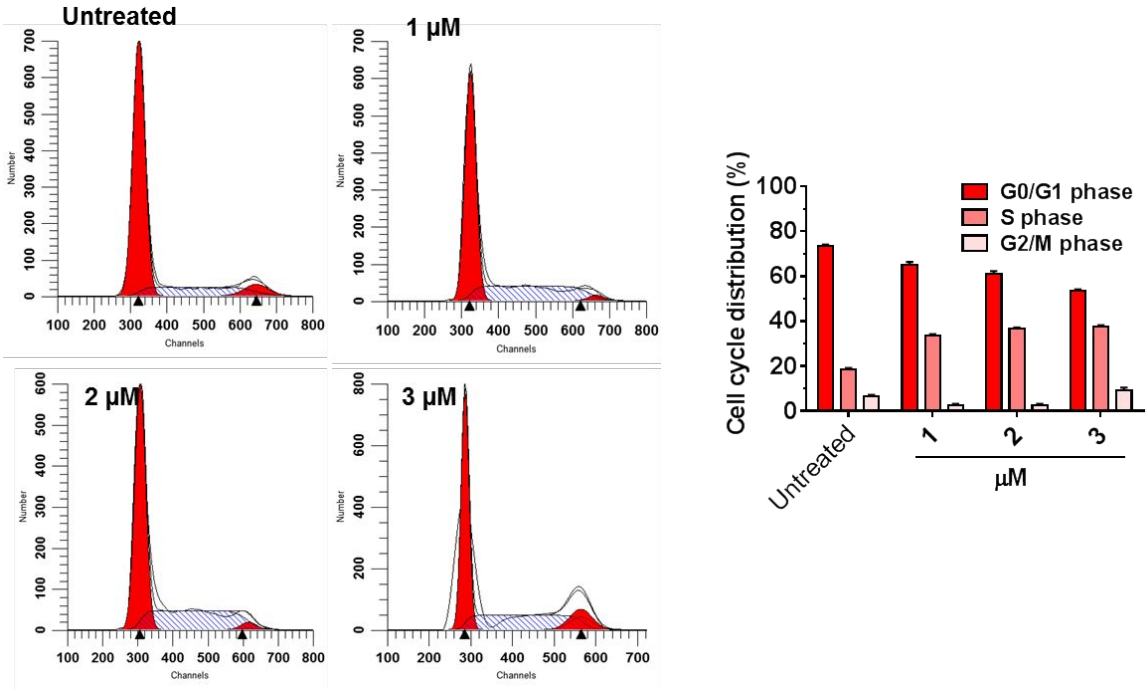

Figure S46. Dose dependent activity of complex **6** in cell cycle distribution by flow cytometry.

References:

1. Bennett M. A.; Smith, A. K. Arene ruthenium(II) complexes formed by dehydrogenation of cyclohexadienes with ruthenium(III) trichloride, *Journal of the Chemical Society, Dalton Transactions,***1974**, 233-241.
2. Bennett, M. A.;Huang,T. N.;Matheson, T. W.; Smith, A. K.; Ittel,S.; Nickerson,W. Some η^5-Cyclopentadienylruthenium(II) Complexes Containing Triphenylphosphine, *Inorg. Synth*., **1982**, 74-78.
3. Vogel, A. I.;*Test book of practical organic chemistry, Longman, London, 5th edn*, **1989**, p.395
4. Sheldrick, G. M.;A short history of SHELX, *Acta Crystallographica Section A,***2008**,*64*, 112-122.
5. Farrugia, L.ORTEP-3 for Windows - a version of ORTEP-III with a Graphical User Interface (GUI), *Journal of Applied Crystallography,***1997**, *30*, 565-566.
6. (a) Gupta, R. K.; Sharma, G.; Pandey, R.; Kumar, A.; Koch, B.; Li, P.-Z.; Xu, Q.; Pandey, D. S. DNA/protein binding, molecular docking, and in vitro anticancer activity of some thioether-dipyrrinato complexes. *Inorg.Chem.,* **2013**, *52*, 13984– 13996. (b) Gupta, R. K.; Pandey, R.; Sharma, G.; Prasad, R.; Koch, B.; Srikrishna, S.; Li, P.-Z.; Xu, Q.; Pandey, D. S. DNA Binding and Anti-Cancer Activity of Redox-Active Heteroleptic Piano-Stool Ru(II), Rh(III), and Ir(III) Complexes Containing 4(2-Methoxypyridyl)phenyldipyrromethene. *Inorg. Chem.,* 2013, 52, 3687-3698. (c) OECD, Guidelines for Testing of Chemicals; OECD: Paris, France, **1995**; Vol. *107*.